Investigating the role of *KCNQ1* and *CFTR* as colorectal cancer tumor suppressors

A Thesis SUBMITTED TO THE FACULTY OF
UNIVERSITY OF MINNESOTA
BY

Fatima Alwan

IN PARTIAL FULFILLMENT OF THE REQUIREMENTS
FOR THE DEGREE OF
MASTER OF SCIENCE

Dr. Patricia Scott, Dr. Robert Cormier

July 2017

Acknowledgements

I would like to first thank my family and friends for their guidance and support throughout my graduate career. I would also like to thank my thesis committee Dr. Scott, Dr. Cormier, and Dr. Holy for their guidance and assistance throughout these projects. Kyle Anderson contributed to this work greatly and taught me so much about being a scientist. None of this work would have been possible without the financial support I received from the Biology department through my GTA appointments and from my advisors in the form of summer RAships.

This work was funded by NCI: 1 R01 CA134759-01A1, R15 CA195061A-01, University of Minnesota AHC Faculty Development Grant, Whiteside Institute for Clinical Research, and Essentia Health Systems. A special thank you to our collaborators at the University of Minnesota Twin Cities, David Largaespada, Tim Starr, Gerry O'Sullivan, Ying Zhang, and Alex Khoruts and our collaborators at the Netherlands Cancer Institute, Amsterdam- Remond Fijneman, Gerrit Meijer, Jeroen Goos, and Sjoerd den Uil.

Dedication

This thesis is dedicated to my family. Without them, I am nothing.

Abstract

Colorectal cancer (CRC) is the second-highest cause of cancer deaths in the United States. A comprehensive understanding of disease development and progression is critical for the advancement of effective diagnostic and treatment methods for CRC patients. Forward genetic screens have identified numerous candidate genes that may be driving tumor development and progression (Starr *et al.* 2009). Two identified candidate genes are potassium voltage-gated channel subfamily Q member 1 (*KCNQ1*) and cystic fibrosis transmembrane conductance regulator (*CFTR*). Previous studies show knockout of *Kcnq1* or *Cftr* alone causes increased intestinal tumorigenesis in the Apc^{Min} mouse model, and low expression of *KCNQ1* or *CFTR* in CRC tumors is associated with poor outcomes in human CRC (Than, *et al*. 2014, 2016). To further investigate the role of these genes as CRC tumor suppressors, we harvested intestinal organoids from *Kcnq1* and *Cftr* knockout (KO) and wild-type (WT) mice and isolated RNA from these organoids. Illumina Next-Generation RNA Sequencing and quantitative reverse-transcriptase PCR was performed using organoid RNA to evaluate and compare gene expression. In addition, preliminary phenotypic characterization of organoids derived from *Kcnq1* and *Cftr* WT and KO mice was performed. Bioinformatic analysis by Gene Set Enrichment Analysis (GSEA) using human cancer datasets further characterized gene expression changes in KCNQ1 and CFTR low-expression phenotypes. Our data show Kcnq1 is localized to the stem cell compartment of the small intestine, and loss of *Kcnq1* and *Cftr* effect gene expression in isolated organoids as well as primary tissue. Loss of these tumor suppressive genes alter specific biological pathways, including cholesterol

biosynthesis and the unfolded protein response, that may lead to cancer development and progression.

Table of Contents

Introduction

Colorectal cancer

Colorectal cancer (CRC) is the second-highest cause of cancer deaths in the United States, resulting in approximately 136,830 new cases nationwide each year and 50,310 deaths per year due to CRC in 2014 (Kasper *et al.* 2012). A comprehensive understanding of disease development and progression is critical for the development of effective diagnostic and treatment methods for CRC patients, which currently are lacking in efficacy. Many benign polyps, adenomas, are detected during routine colonoscopies and such polyps can be surgically removed. Individuals diagnosed with early stage CRC (Stages I and II) are often considered cured by surgery alone and do not receive adjuvant chemotherapy. Stage I cancers consist of superficial epithelial lesions that have not invaded nearby lymph nodes and have begun to penetrate the underlying submucosa (Kasper *et al.* 2012). Colorectal cancer is diagnosed as Stage II if there are tumors present that penetrate through the muscularis of the tissue, but have not yet completely invaded the muscularis and have not spread to regional lymph nodes (Harrison's). However, 25% of Stage II patients experience disease relapse and die within 5 years. There is currently no method of identifying these and other at-risk individuals. Later stages of CRC become more difficult to treat, as they are defined as cancers that have spread to the regional lymph nodes (Stage III) or as cancers that have metastasized to distant sites such as the liver or lung (Stage IV). Surgical resection of affected organs is a possible treatment for Stage IV patients, but 5-year survival is below 30%. Due to the unacceptable survival rates of Stage IV patients, there is an urgent need for new therapies. Currently, gaps in

our knowledge prevent us from developing more efficient diagnosis and treatment measures, both to identify patients at higher risk for relapse and thus in need of increased disease surveillance and more aggressive treatment, and for patients suffering from the later stages of cancer (III and IV). Research to determine the functional mechanisms underlying CRC development as well as identifying potential prognostic and diagnostic biomarkers will greatly contribute to the effort to establish more effective diagnosis and treatment.

The Intestinal Stem Cell Compartment

Colorectal cancer arises from the intestinal epithelium. Small intestinal tissue is composed of crypts and villi (Figure 1), while the large intestinal tissue lacks the absorptive villi. At the base of the crypt compartment reside five to six self-renewing stem cells (Sato *et al.*, 2009). These cells produce transit amplifying progenitor cells, which proliferate but may only divide several times before differentiating (Sato *et al.*, 2009). Differentiated cells that result from progenitor cells include enterocytes, goblet cells, Paneth cells (not present in the colon), and enteroendocrine cells (Sato *et al.*, 2009).

In the small intestine, epithelial cells form villi, with rapidly dividing cells from the crypt bottom pushing and shedding older, apoptotic cells near the tip of the villi. Apoptosis occurs approximately three days after epithelial cells differentiate and migrate upwards (Sato *et al.*, 2009). Paneth cells do not migrate upwards, but remain in contact with stem cells near the base of the crypt and are responsible for maintaining the microenvironment of stem cells (Sato *et al.*, 2009).

On average, an individual epithelial cell's life cycle is less than a week long, and in the mouse, approximately 200 new cells are generated per crypt each day (Reya and Clevers, 2005). In the adult intestinal tissue, progenitor proliferation, cell differentiation, and apoptosis are regulated by stem cells in the crypt compartment (van der Flier and Clevers, 2009). These stem cells reside in a tightly regulated microenvironment. The stem cell niche is formed by the subepithelial myofibroblasts, which secrete various growth factors and cytokines to promote proliferation of the epithelium (van der Flier and Clevers, 2009). The tight regulation and cross-talk between stem cells, Paneth cells in the small intestine and Paneth-like cells in the large intestine, and the underlying mesenchyme maintains the delicate homeostasis of the tissue in regards to proliferation, differentiation, and apoptosis. Dysregulation of these cellular signals leads to abnormal growth, and in some cases, colon cancer.

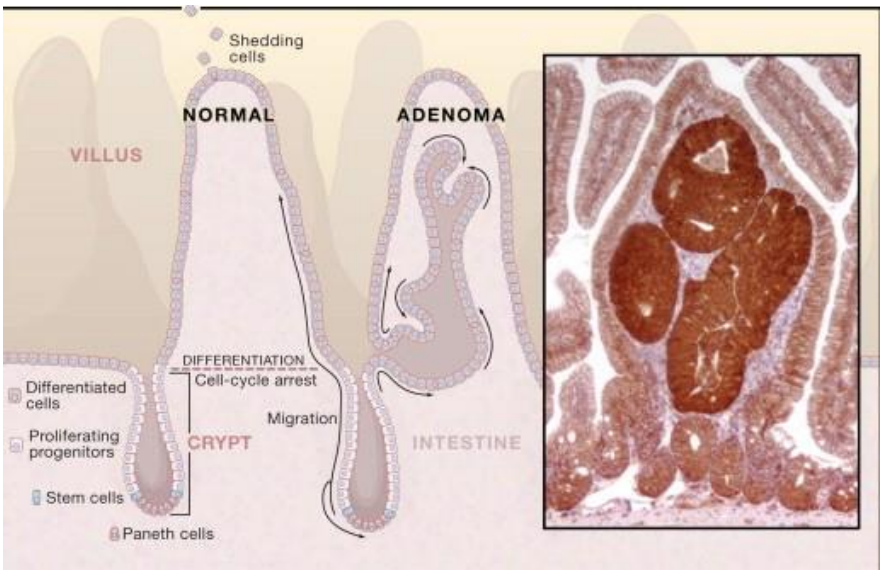

Figure 1 Intestinal stem cells directing proliferation of progenitor cells and the formation of the villi, in normal versus adenoma tissue (Clevers, 2006).

Molecular Regulation of the Intestinal Tissue

Homeostasis of intestinal tissue is tightly controlled by multiple signaling pathways (Sato and Clevers, 2013). Signaling pathways create a feedback that maintains the balance between cell proliferation, and apoptosis in a tissue that experiences complete turnover very rapidly. In addition, these signaling pathways direct progenitor cells to cell lineage specification, resulting in the differentiation of cells to the secretory lineage (Paneth cells, goblet cells, and enteroendocrine cells) or the absorptive lineage (enterocytes) (van der Flier and Clevers, 2009).

The Wnt/β-Catenin canonical signaling pathway is highly conserved and is crucial for growth and patterning during development (Farin *et al.*, 2016). Although the mechanism of Wnt protein secretion and signaling is well-developed in *Drosophila*, limited information exists on endogenous Wnt protein distribution in vertebrates (Farin *et al.*, 2016). Wnt is structurally unique due to its insolubility, high number of cysteine residues, and covalently attached N-terminal fatty acid chain, which increases its binding to cellular surfaces (Clevers, 2006). In the intestinal crypt, stem cell self-renewal, proliferation, and differentiation are coordinated along a Wnt gradient (Farin *et al.*, 2016). Wnt is secreted by Paneth cells and travels away from its source in a cell-bound manner via cell diffusion, leading to the establishment of the Wnt gradient along the crypt (Farin *et al.* 2016). Wnt binds to its cognate Frizzled receptors on neighboring stem cells, where its signaling cascade leads to activation of Wnt target genes.

Wnt is the primary driving force behind proliferation of epithelial cells in the intestine. The canonical Wnt/β-Catenin pathway is activated upon Wnt binding to Frizzled transmembrane receptor proteins. This binding interaction recruits additional

transmembrane molecules LRP5 and -6 and Mesd to Frizzled, which further activates the signaling cascade (Clevers, 2006). Once Frizzled-LRP is bound by its ligands, Frizzled interacts with the cytoplasmic protein Dishevelled. Wnt binding to Frizzled/LRP also induces the phosphorylation of the cytoplasmic tail of LRP, which allows for the docking of the cytoplasmic Axin protein. Phosphorylation of Axin by CK1 family kinases promotes the Dishevelled and Axin heterodimer to cooperatively mediate downstream signaling activation events. β-Catenin is the key effector of the canonical Wnt pathway signaling cascade. In the presence of Wnt, the tumor suppressor protein Axin is phosphorylated and bound in its heterodimeric state at the membrane, preventing its interaction with β-Catenin and the Adenomatous Polyposis Coli (APC) protein. The recruitment of Axin away from the APC destruction complex prevents the degradation of β-Catenin by the destruction complex, thus allowing β-Catenin to translocate to the nucleus, where it dislocates the transcriptional repressor Groucho from TCF to promote the transcription of Wnt target genes. In the absence of Wnt, Axin binds to the APC and β-Catenin complex, initiating the phosphorylation of β-Catenin by CK1 kinases, which consequently target β-Catenin for ubiquination and degradation by the proteasome. This prevents the translocation of β-Catenin to the nucleus and the subsequent transcription of Wnt target genes. (Clevers, 2006 and Clevers, 2005, and Clevers, 2012) (Figure 2).

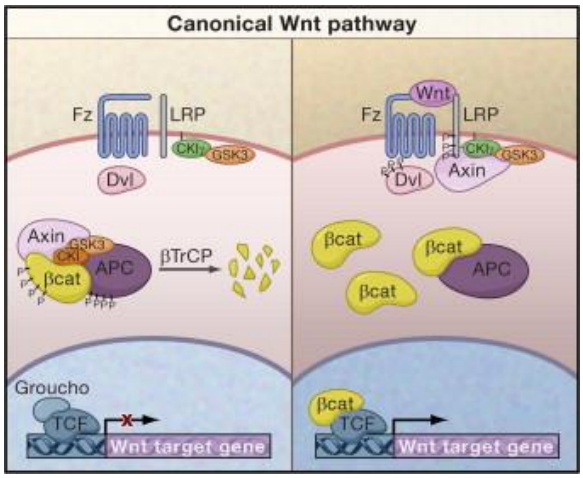

Figure 2. Wnt signaling stimulates transcription of target genes by β-Catenin activation, while the absence of Wnt signaling inhibits transcription of these genes. Abbreviations in the figure: β-Cat- β-Catenin, APC- Adenomatous Polyposis Coli, Fz- Frizzled.

The transcriptional programs activated by Wnt signaling have been described as necessary for the maintenance and activation of stem cells in the intestinal epithelium (Reya and Clevers, 2005). Wnt target genes promote cell proliferation and tissue expansion as well as cell fate determination (Reya and Clevers, 2005). A study of neonatal transgenic *Tcf4*$^{-/-}$ mice showed that the absence of this transcriptional activator that is regulated by Wnt signaling did not affect the villus of the epithelial compartment, but obliterated the crypt progenitor compartment (Reya and Clevers, 2005). These results suggest Wnt signaling is required for maintenance of the crypt progenitor phenotype, and is a positive feedback on epithelial stemness.

The Wnt pathway is of interest in colorectal cancer because mutation of the *APC* gene is found in 90% of sporadic colorectal carcinomas (Kinzler and Vogelstein, 1996). The APC protein constrains Wnt/β-catenin signaling by mediating the degradation of β-catenin by the proteasome in the cytoplasm (Clevers, 2006). Loss of this degradation function results in an excess of β-catenin and increased transcription of genes controlling

epithelial stemness. This causes uncontrolled expansion of the stem cell population and results in a drastic increase in the number and size of intestinal crypts (Reya and Clevers, 2005). Heterozygosity of *APC* in mice and humans, when coupled with an additional somatic mutation of *APC*, causes an expansion of progenitor cells in the crypt, resulting in adenomatous tissue development in the intestine (Sansom *et al.*, 2004). The Apc^{Min} mouse carries one inherited germline defective allele of *Apc* and is a common experimental model for colorectal cancer, as it provides a genetic background that provides an activating mutation of the Wnt cascade, which current evidence suggests is an initiating event in CRC development (Reya and Clevers, 2006).

Notch signaling is also involved in the feedback that maintains homeostasis of intestinal tissue. The Notch pathway is important for intestinal cell fate decisions, as it directs the differentiation of secretory cell lineages. Like Wnt signaling, the Notch pathway is essential for the maintenance of the undifferentiated and proliferative state of the crypt compartment (van der Fliers and Clevers, 2009). It is known that Notch regulates cell differentiation and plays a role in tumorigenesis, but our understanding of the mechanism is poor. In colorectal cancer, altered feedback from Notch prevents cells from progressing to their differentiated state (van der Flier and Clevers, 2009). Undifferentiated cells can form tumors, eventually resulting in cancerous growth (van der Flier and Clevers, 2009). Upon activation, Notch undergoes a proteolytic cleavage and translocates to the nucleus of the cell where it acts as a transcription factor to turn on expression of target genes (Sikandar *et al.*, 2010). Inhibition of this signaling in mice results in a negative feedback of maintenance of epithelial stemness, and an increase in

the goblet cell population (Sikandar *et al.*, 2010). Notch signaling plays an important role in the initiation of tumors, as it is a positive feedback on stemness (lack of differentiation and proliferation) (Sikandar *et al.*, 2010).

Bone morphogenic protein (BMP) provides negative feedback on intestinal stem cell self-renewal (He *et al.*, 2004). Although the exact mechanism is not fully understood, inactivation of BMP in mice alters intestinal tissue homeostasis and increases stem cell and progenitor cell populations, eventually leading to polyposis (He *et al.*, 2004), supporting BMP's function as a stem cell inactivator. BMP normally functions by suppression of Wnt signaling, thus and creating a negative feedback on stem cell self-renewal (He *et al.*, 2004). Noggin is a secondary signaling molecule which inhibits the action of BMP, preventing the inhibition of Wnt. BMP is secreted by neighboring Paneth cells in response to increased stem cell proliferation; its signal then inhibits Wnt, creating a negative feedback loop on epithelial stemness.

Wnt, Notch, and BMP constitute a feedback system that is necessary for maintenance of homeostasis between cell proliferation, differentiation, and cell death. Cancer is the result of disruption of this homeostasis, via alteration of the many signaling pathways that set up this feedback. How one signaling pathway affects another is not fully understood, although relationships have been implied (Sikandar *et al.*, 2010).

Genetic factors contributing to colorectal cancer development

Colorectal cancer is a disease of genetic alterations that often develops over decades and requires several genetic changes to be considered malignant, which is characterized by uncontrolled growth (Kinzler and Vogelstein, 1996). Colorectal cancers

can be classified as inherited and sporadic. Inherited dominant predisposition syndromes are estimated to account for approximately 5% of CRC, and Familial Adenomatous Polyposis accounts for 0.5-1% of total cases (Kinzler and Vogelstein, 1996). Familial Adenomatous Polyposis (FAP) is a highly penetrant, autosomal dominant syndrome that results from the germline mutation of the Adenomatous Polyposis Coli (*APC*) gene and affects 1 in 7,000 individuals (Kinzler and Vogelstein, 1996). FAP patients develop hundreds to thousands of benign colorectal polyps that often develop into cancerous lesions (Kinzler and Vogelstein, 1996). FAP is important to our overall understanding of CRC because the causal genetic defect affects the rate of tumor formation by altering a key gatekeeper gene, *APC* (Kinzler and Vogelstein, 1996). *APC* is also mutated in ~80% of sporadic cases of CRC; thus, better understanding its role in FAP will lend to an understanding of colon cancer tumorigenesis overall.

CRCs are further classified by their genetic instability as either microsatellite instable or chromosomal instable. Microsatellite instability is caused by defects in the cellular mismatch repair machinery and has been widely studied in many tumor types (Fodde *et al.*, 2001). Chromosomal instability is characterized as tumors that exhibit defective chromosomal segregation during cell division, which leads to variation in chromosome numbers (aneuploidy) among cells from individual clones (Fodde *et al.*, 2001). The seminal work investigating the genetic alterations of colon cancers found that somatic mutations of KRAS, APC, and P53 were present in most colon cancers, both familial and sporadic (Bos *et al.*, 1987; Baker *et al.*, 1990; Cho and Vogelstein, 1992). Despite these common limiting genetic mutations or epigenetic alterations, every

individual CRC case exhibits as many as a hundred or more mutations, while only a few (an estimated 10-20) are causally involved in cancer development. These mutations cause CRC by dysregulating important biological processes and many key cellular signaling pathways (Saif and Chu, 2010).

Sleeping Beauty Transposon Mutagenesis Identified Colorectal Cancer Candidate Genes

A common and powerful tool for cancer gene identification is forward genetic screens in mice utilizing transposons, which are DNA elements that translocate randomly throughout the host genome. Mutagenesis by transposon insertion allows for the unbiased discovery of novel candidate cancer genes. The genetic changes of human colorectal cancers are varied, with respect to both genetic and epigenetic alterations. Starr *et al.* utilized a *Sleeping Beauty* (SB) system to identify which genetic alterations are causally involved in intestinal tumorigenesis (drivers) and which have little functional impact in cancer development (passengers) (Starr *et al.*, 2009). To identify these driver genes, Starr *et al.* inserted mutagenic SB11 transposase cDNA preceded by a LoxP-flanked stop cassette into the Rosa26 locus, then crossed these transgenic mice to *Villin-Cre* transgenic mice to restrict transposase activation to the gastrointestinal tract epithelium (Starr *et al.*, 2009). When expressed, the SB transposase activated the transposition of the mutagenic transposon *T2/Onc*, which contains a murine stem cell virus long terminal repeat and splice donor site (Starr *et al.*, 2009). This characteristic of *T2/Onc* can deregulate the expression of a proto-oncogene. On the other hand, *T2/Onc* also has splice acceptor sites and a bidirectional poly(A) signal which can inactivate the expression of a tumor suppressor gene (Starr *et al.*, 2009). Mice that developed tumors were sacrificed,

and DNA was isolated and sequenced from those tumors to identify common insertion sites of the transposon, which are defined as insertion sites which occurred at a higher rate than that which is expected due to random chance (Starr *et al.*, 2009). These candidate driver genes were suspected to be involved in colorectal cancer, and thus it is crucial to first determine whether these genes are causally involved in cancer development, and whether this involvement is tumor suppressive or oncogenic. Furthermore, two of these candidate genes, *KCNQ1* and *CFTR*, were used to inform the specific gene targets of this thesis.

KCNQ1

KCNQ1 Physiological Function

The *KCNQ1* gene encodes a voltage-gated potassium channel widely expressed throughout the body, including the myocardium, inner ear, stomach, pancreas, and intestine (Than *et al.*, 2013). The KCNQ1 channel protein is composed of six transmembrane-spanning α-helices and a pore loop, with typical potassium channel pore signature sequence structure. KCNQ1 is a voltage-gated channel opened by increasing membrane depolarizations. Once opened, the channel creates slowly activating and deactivating potassium currents (Jespersen *et al.*, 2005).

KCNQ1 is a key regulator of ion homeostasis and modulates water and salt transport in epithelial tissues. The epithelium serves as a functional barrier between the external and internal environment, and transport of substances through this barrier is dependent on the activity of channels. Potassium channels, such as KCNQ1, maintain a membrane potential necessary for transepithelial transport. KCNQ1 is expressed in many

epithelial tissues and has been demonstrated to modulate transepithelial transport as well as the secretion of potassium (Diener *et al.*, 1996).

KCNQ1 channels secrete potassium across the basolateral membrane in the intestinal epithelium. Continuous transepithelial transport is dependent on basolateral potassium conductance modulated by KCNQ1. Chloride enters the basolateral membrane by cotransport with potassium and sodium, and is subsequently secreted through CFTR chloride channels located on the apical membrane. This secretion is dependent on basolateral potassium conductance, which is modulated in part by KCNQ1.

In the mouse small intestine expression of Kcnq1 occurs in a gradient, with the highest expression in the duodenum and proximal jejunum and the lowest expression in the ileum (Demolombe *et al.*, 2001; Dedek and Waldegger, 2001). In the mouse large intestine, Kcnq1 expression is highest in the distal colon (Vallon *et al.*, 2005; Warth *et al.*, 2002). On the cellular level, Kcnq1 is expressed in the base of the intestinal crypt (Fig. 1, Alwan, unpublished data). The localization and expression of KCNQ1 in the intestinal epithelium suggests a role for the regulation of intestinal stem cells, which are also located at the base of the crypt.

KCNQ1, Ion Channels, and Cancer

Ion transporters and the voltage gradients they create are involved in development and proliferation (Morokuma *et al.*, 2008). Ion channels regulate the microenvironment of stem and tumor cells, thus regulating their behavior (Morokuma *et al.*, 2008). Stem cells of the intestinal crypt receive signals from their environment. These signals include

not only ligands (such as Wnt, Notch, and BMP), but also those of electrical nature, such as ion currents and voltage gradients (Morokuma *et al.*, 2008).

Voltage-gated potassium channels functionally regulate progression through the cell cycle (Blackiston *et al.*, 2009). Molecular physiology studies show other voltage-gated K^+ channels are inhibited upon cell maturation (Kunzelmann, 2005). But, cancerous cells maintain the activity of these ion channels and highly express them past cell maturation, which increases proliferation (Kunzelmann, 2005). Mutation of *KCNQ1* disrupts ion homeostasis and may alter the complex signaling required for normal cell proliferation. Identifying if and how this change in ion conductance causes oncogenic phenotypes in intestinal epithelium is key to a comprehensive understanding of CRC.

Evidence Supporting KCNQ1 as a Tumor Suppressor in Colorectal Cancer

KCNQ1 is a colorectal cancer tumor suppressor gene. A *Sleeping Beauty* DNA transposon mutagenesis screen of intestinal epithelial cells in wildtype mice revealed *KCNQ1* as a candidate driver gene for intestinal tumorigenesis, as the gene was identified as a high frequency common insertion site locus (Starr *et al.*, 2009). In addition, another genetic screen in Apc^{Min} mice by Starr *et al.* (2011) found *Kcnq1* mutations in 13% of intestinal tumors analyzed, ranking it as one of the top ten common insertion site genes of these genetic screens (Starr *et al.*, 2011). Loss of *Kcnq1* promoted tumor progression and enhanced tumor multiplicity in Apc^{Min} mice by approximately two-fold in the proximal small intestine and colon. cDNA microarray expression studies of distal colon and small intestine tissue derived from *Kcnq1* knockout mice showed loss of *Kcnq1* had a strong effect on gene expression. Pathways affected by loss of *Kcnq1* included intestinal stem

cell-related genes, suggesting further that *Kcnq1* is a tumor suppressor by having a role in the intestinal stem cell compartment (Than *et al.*, 2013).

Additionally, clinical data suggests *KCNQ1* is a tumor suppressor in colon cancer. Microarray gene expression data used to analyze *KCNQ1* mRNA expression in 90 stage II colon cancer patients found that low expression of *KCNQ1* was associated with poor disease-free survival (den Uil *et al.*, 2016). In the same study, *KCNQ1* protein expression was analyzed in a cohort of 386 stage II and stage III colon cancer patients by immunohistochemistry of tissue microarrays. These studies found that *KCNQ1* may be a viable biomarker for prediction of disease recurrence (Starr *et al.*, 2009). A Kaplan-Meier plot comparing high *KCNQ1* expression and low *KCNQ1* expression in colon cancer patients against overall survival after hemihepatectomy correlated expression of *KCNQI* and survival time of late-stage CRC, with a substantial survival difference of 23 months longer in *KCNQ1* high expressing CRC patients (Than *et al.*, 2013).

CFTR

Another gene identified as a candidate driver gene of colorectal cancer in a *Sleeping Beauty* Transposon Mutagenesis screen is the cystic fibrosis transmembrane conductance regulator (*CFTR*) (Starr *et al.*, 2009). *CFTR* encodes an epithelial anion channel and mutations of this gene cause cystic fibrosis (CF), a disease which affects about 85,000 people worldwide (Bell *et al.*, 2015). CF patients have altered gastrointestinal physiology due to deficient anion and fluid transport, including altered cellular pH, impaired release and elimination of mucus, abnormal microbiota colonization, and dysregulated innate immune responses that lead to inflammation (De

Lisle and Borowitz, 2013). Considering these alterations in gastrointestinal physiology, it is not surprising that a 20-year cohort study of CF patients in the United States found these patients have an increased risk of developing gastrointestinal cancers (Maisonneuve *et al.*, 2013).

CFTR is a cyclic AMP-dependent transporter of Cl^- and HCO_3^- in the crypt epithelium, where it is most highly expressed in the base of the crypt and is present at reduced levels in the villous epithelium (Liu *et al.*, 2012). *CFTR* was of interest to our lab as a candidate gene because the protein's function is dependent on the function of KCNQ1 as KCNQ1 creates a potassium current that enables the dependent Cl^- section by CFTR. Together, these ion channels play multifunctional roles in processes of ion and acid-base transport that are essential to normal crypt physiology (Liu *et al.*, 2012).

Published data by our lab as well as other researchers suggest a role for CFTR as a tumor suppressor gene in colorectal cancer. Than *et al.* examined CFTR deficiency in mouse models and human CRC patients to confirm its role in CRC development implied by previous *Sleeping Beauty* screens. Their data show that loss of *Cftr* significantly enhances tumor multiplicity in both the small intestine and colon in the Apc^{Min} mouse model (in both heterozygous and homozygous mutants). Loss of *Cftr* alone also induced tumor formation in both the colon and small intestine of mice, with a >60% penetrance. Loss of *CFTR* expression in stage II CRC human patients showed similar effects, as 3-year relapse-free survival was 85% in the *CFTR* high-expressing group, compared to 56% in the *CFTR* low-expressing group (Than *et al.*, 2016). Considered together, these

results confirm the role of *CFTR* as a CRC tumor suppressor gene, although the data does not inform on the functional mechanism of tumor suppression.

Biological Pathways of Interest

Many biological pathways may influence or play a role in the development of colorectal cancer. Specifically, dysregulation in the form of activation or repression of normal cellular responses contributes to the development and progression of CRC. The identification of these altered pathways as well as the characterization of their oncogenic or tumor suppressive effects helps establish a model of CRC carcinogenesis, and can lead to the development of more effective treatment and diagnostic measures. Analysis of *CFTR* normal and deficient tissue by Ingenuity Pathway Analysis (IPA) revealed the LXR/RXR pathway as an altered pathway due to loss of *CFTR* expression. Similarly, analysis of *Kcnq1*-deficient organoids by Gene Set Enrichment Analysis (GSEA) revealed the unfolded protein response (UPR) was altered due to loss of *Kcnq1* expression. These two pathways were explored further in this thesis.

The Unfolded Protein Response

A known pathway altered in multiple cancers is the unfolded protein response, a highly conserved process among taxa initiated in response to endoplasmic reticulum (ER) stress due to the accumulation of misfolded proteins. Misfolded proteins in the ER lumen are detected by glucose regulated protein 78 (grp78), a chaperone and negative regulator of PERK, IRE1, and ATF6 (Kaser *et al.*, 2010). Grp78 binds misfolded proteins in the lumen of the ER as well as PERK, IRE1, and ATF6, until the chaperoning capacity of the protein is exceeded, in which case the unfolded protein response is activated by Grp78

releasing its binding to PERK, IRE1, and ATF6 to instead bind misfolded proteins, releasing the inhibition of the three arms of the effector pathway (Kaser *et al.*, 2011). The unfolded protein response is initiated by three main signaling pathways; pancreatic ER kinase (PERK), activation transcription factor 6 (ATF6), and inositol requiring enzyme 1 (IRE1) (Kaser *et al.*, 2010). Upon initiation of these signaling pathways, respective transcription factors are activated and translocate to the nucleus, where they direct a transcriptional program to direct the cellular response to the accumulation of misfolded proteins and its consequences (Kaser *et al.*, 2010).

The three effector arms, PERK, IRE1, and ATF6, lead to defined transcriptional changes that ultimately comprise the unfolded protein response. Upon activation by sensing the presence of unfolded proteins, the kinase function of PERK is activated and elongation initiation factor 2α (elF2α) is phosphorylated (Harding *et al.*, 2000). elF2α is a translation initiation factor that is unable to bind in its phosphorylated state, resulting in a halt in protein synthesis (Harding *et al.*, 2000). However, activation factor 4 (ATF4) is not inhibited by elF2α and directs the transcription of the CCAAT/enhancer binding homologous protein (CHOP), which promotes cell death (Vattem *et al.*, 2004). ATF6 is activated by the detection of misfolded proteins in the ER lumen and subsequently translocates to the Golgi apparatus, where its transcriptionally active cytoplasmic tail is cleaved and directs a transcriptional response to ER stress (Todd *et al.*, 2008 and Haze *et al.*, 1999). The final arm of the unfolded protein response, IRE1, dimerizes and autophosphorylates upon activation. Two main forms of IRE1 are expressed in mammals: IRE1α is ubiquitously expressed, while IRE1β expression is restricted to the intestinal

epithelium (Cao and Kaufman, 2012). In its activated form IRE1 cleaves the transcription factor XPB1 which causes the transcription factor to be spliced and activated. IRE1 functions as an endoribonuclease and kinase (Cao and Kaufman, 2012). These pathways are illustrated below in Figure 3.

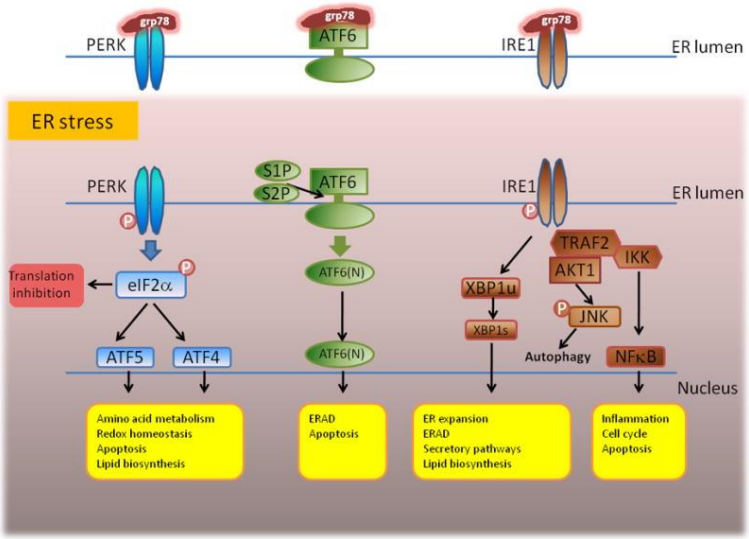

Figure 3. The three arms of the unfolded protein response- PERK, ATF6, and IRE1. (Kaser *et al.*, 2011, Exp. Cell Research.)

The Unfolded Protein Response and Disease

Endoplasmic reticulum stress can be caused by a variety of factors, both intrinsic and extrinsic. The most common physiological factor that leads to ER stress is simply an increase in protein synthesis, which could be due to cell stimulation by growth factors, cell proliferation, differentiation, or senescence (Wang and Kaufman, 2016). In addition to these normal cellular stressors, mutations in protein folding genes or defects in UPR signaling can induce ER stress (Wang and Kaufman, 2016). The ability of a cell to manage ER stress via the UPR is crucial for the maintenance of homeostasis, and thus

disruption of these processes can lead to various disease states. Pathologic conditions cause changes in the microenvironment that may induce ER stress independently or in addition to normal biological stressors, such as inflammation, hypoxia, or nutrient deprivation (Wang and Kaufman, 2016). Considering these factors, it is unsurprising that ER stress has been found to contribute to the initiation and progression of numerous diseases in humans, including neurodegenerative disease, metabolic disease, inflammation, and cancer (Wang and Kaufman, 2016).

Previous studies have shown ER stress-related genes and proteins display altered expression in cancers (Moenner *et al.*, 2007). For example, the expression of ER chaperone glucose-regulated protein (GRP) 78/BiP and GRP 94 have been found to be altered in at least ten different cancers, including colorectal cancer (Moenner *et al.*, 2007). Grp78 directly plays a role in the ability of cells to resist proapoptotic challenges, implying its influence in cancer development and progression (Moenner *et al.*, 2007). The UPR is of interest in cancers that involve secretory cells, such as colorectal cancer, which originates from the highly secretory columnar epithelium that lines all mucosal surfaces (Kaser *et al.*, 2011). Highly secretory cells (such as Goblet and Paneth cells in the intestinal epithelium) are especially vulnerable to ER stress and as such are dependent on a functional UPR for homeostasis (Kaser *et al.*, 2011).

In addition to the defined UPR role in homeostasis, recent studies have shown UPR activity is involved in cell fate decisions (van Lidth de Jeude *et al.*, 2016). Colorectal cancer develops from oncogenic mutations that occur in intestinal stem cells, which direct and regulate cell proliferation, apoptosis, and differentiation in the tissue.

Because cancer develops from dysregulation of intestinal stem cells, studies have aimed to directly evaluate the effect of ER stress on stem cells and cell differentiation in the intestinal epithelium. During normal cell differentiation, a multitude of transmembrane and secreted proteins are produced in the ER, which attracts chaperones such as Grp78 and shifts them away from their bound position on the three transmembrane UPR receptors IRE1α, ATF6, and PERK (Ni and Lee, 2007). These receptors then activate the UPR by their respective signaling pathways. A study of the intestinal epithelium by Heijmans *et al.* using genetic and cellular techniques revealed that levels of ER stress and UPR activation are low in intestinal stem cells compared to differentiated transit amplifying cells (2013). This study also demonstrated that activation of Perk-elF2α signaling alone induces intestinal epithelial stem cell differentiation. The data from Heijmans *et al.* show differential activity of ER stress between stem cells and transit-amplifying cells in the intestinal epithelium, which suggests the ER may regulate intestinal epithelial stem cell differentiation.

To investigate the function of ER stress and UPR induction in intestinal epithelium that has already acquired oncogenic mutations, van Lidth de Jeude *et al.* (2016) generated transgenic mice in which *Apc* and *Grp78* could be conditionally knocked-out and harvested intestinal organoids from these mice. As previously described, *Apc* is an important tumor suppressor gene for colorectal cancer and is a negative regulator of the Wnt/β-catenin pathway. van Lidth de Jeude *et al.* found that loss of *Apc* alone resulted in crypt elongation, activation of the Wnt signature, and accumulation of intestinal stem cells (2016). This phenotype was completely rescued upon activation of

ER stress by additional deletion of *Grp78*. In *Grp78 Apc* double knockout mice, stem cells were lost and repopulation occurred by non-mutant cells only, which implies these double-knockout mice had lost the capacity to self-regenerate (2016). These results, along with others, suggest an important role for ER stress and the UPR in regulating intestinal stem cell differentiation. Understanding how these biological processes are involved in inducing differentiation could lead to functional information about the mechanisms of CRC development and progression, and may also be a promising therapeutic target.

Cholesterol Biosynthesis and Homeostasis

Cholesterol biosynthesis and homeostasis are crucial for normal cell functioning as cholesterol is an important component of cell membranes and is involved in many other biological processes. The association between cholesterol metabolism and cancer has been thoroughly investigated and it has been shown that proliferating cells increase cholesterol uptake. Hyper-proliferative cancer cells maintain high intracellular cholesterol through various mechanisms including accelerated endogenous production of cholesterol and fatty acids and reduction of cholesterol efflux via membrane transporters. The dependency of rapidly proliferating cells on cholesterol biosynthesis and homeostasis mechanisms has made this a promising and interesting target for cancer research (Gabitova *et al.*, 2014).

Cholesterol metabolites interact with several nuclear receptors, which when bound by their small lipophilic cognate ligands modulate transcriptional activities. Receptors classified in the nuclear receptor superfamily share similar structural

organization and contain an N-terminal activating domain, a DNA-binding domain, a ligand-binding domain, and a C-terminal activating domain (Moschetta, 2015). The liver X receptor (LXR) is a member of the nuclear receptor family and is an established ligand-activated transcription factor. LXRs exist as two isoforms, LXRα, encoded by the gene *NR1H3*, and LXRβ, encoded by the gene *NR1H2* (Vedin *et al.*, 2013). LXRβ is ubiquitously expressed, while LXRα is selectively expressed in metabolically active tissues (Bovenga *et al.*, 2015). In the small intestine and colon both LXR isoforms are highly expressed (Vedin *et al.*, 2013).

LXRs are activated by a metabolite of cholesterol, oxysterol, and regulate the expression of genes involved in lipid, cholesterol, and carbohydrate metabolism (Vedin *et al.*, 2013). When bound to its cognate ligand, LXR binds to LXR response elements and forms a heterodimer with retinoid X receptors (RXRs), which causes a conformational change that recruits additional co-activators to displace co-repressors. This opens the chromatin structure and allows for assembly of the transcriptional machinery, and thus activates transcription of target genes. In the absence of the oxysterol ligand, the heterodimer recruits co-repressor complexes, and transcription of LXR target genes is inactivated (Moschetta, 2015). LXRs act as global cholesterol sensors, and their activation leads to a net reduction of cholesterol by promoting its efflux, limiting its absorption, reducing its cellular uptake, and enhancing its conversion to bile acids in mice (Bovenga *et al.*, 2015). These LXR-mediated responses play an important role in regulating cholesterol metabolism and homeostasis and are thus interesting targets for further investigation of how cholesterol is involved in disease states, particularly cancer.

LXR Activation and Cholesterol Metabolism in Cancer

Epidemiologic studies associate a high-cholesterol diet to an increased risk of colorectal cancer, and it has been well-established that cholesterol controls cell proliferation, as cholesterol is an integral part of the cellular membrane (Lo Sasso *et al.*, 2013). Changes in cholesterol homeostasis have been observed in many tumors (Vedin *et al.*, 2013). Considering this, it is not surprising that disruption of cholesterol metabolism has been associated with the development of cancers, specifically CRC (Lo Sasso *et al.*, 2013). LXRs regulate cholesterol levels by directing transcriptional programs to decrease cholesterol absorption and increase metabolism and excretion of cholesterol, resulting in a net cellular decrease of cholesterol. Thus, numerous studies have evaluated the relationship between LXR activation and tumorigenesis. Lo Sasso *et al.* analyzed the development of colon cancer in mice that express a constitutively active form of LXRα in the intestinal epithelium as well as the development of colon cancer in these mice crossed with Apc^{Min} mice (2013). Proliferation and apoptosis of the human cancer cell line HT29 transfected with Ad VP16hLXRα (an adenoviral vector that expresses LXRα) were compared to a control after ligand-induced activation of LXR with GW3965 (Lo Sasso *et al.*, 2013). Their data show that LXR activation in HT29 human colon cancer cells inhibited the G1 phase of the cell cycle, increased apoptosis, and slowed growth of xenograft tumors in mice compared to control (Lo Sasso *et al.*, 2013). The Apc^{Min} and LXRα double-knockout mutant mice developed fewer and smaller intestinal tumors than control Apc^{Min} mice (Lo Sasso *et al.*, 2013). These results suggest LXR activation

protects against intestinal tumorigenesis, and provide an impetus for further study of the role of this nuclear receptor in CRC development and progression.

Vedin *et al.* further investigated the anti-proliferative mechanism of LXRs in the colon. Their study of human colorectal adenocarcinoma cell lines Colo205 and HCT116 found that activation of both isoforms of LXR, α and β, decreased proliferation of these cancer cells and observed increased expression of proliferation markers in LXRαβ$^{-/-}$ mice (Vedin *et al.*, 2013). In addition, wild-type mice given the GW3965 LXR agonist showed a significant reduction of Ki67, a proliferation marker (Vedin *et al.*, 2013). Their data show that the molecular mechanism underlying the anti-proliferative functions of LXRs is mediated by the ability of LXRs to induce negative cell cycle regulator expression and reduce positive cell cycle regulator expression (Vedin *et al.*, 2013). They also found that activation of LXRs led to hypo-phosphorylation of the Rb protein, and important CRC tumor suppressor protein known to be dysregulated in many cancers (Vedin *et al.*, 2013). These results further confirm the anti-proliferative role of LXRs in the colon, and suggest the mechanism of this suppression is by direct regulation of cell cycle.

As previously discussed in this thesis, β-catenin is a key mediator of the canonical Wnt pathway, which regulates cellular renewal of the intestinal epithelium. To further study the association between liver X receptors and colon carcinogenesis, Uno *et al.* evaluated the effects of LXR activation on β-catenin (2009). Their data show LXR activation decreased mRNA levels of β-catenin transcriptional targets *MYC*, *MMP7*, and *BMP4*, suggesting LXR activation suppresses the activation activity of β-catenin (Uno *et al.*, 2009). This data suggests a molecular link between dietary lipid signaling and

intestinal proliferation pathways, providing a possible explanation for the epidemiologic observation that diet affects colon cancer development (Uno *et al.*, 2009). Because diet is a relatively simple thing to change, it is of interest to further investigate this as a possible CRC prevention or treatment measure.

The accumulating evidence that supports the involvement of LXRs in cancer by regulating cell proliferation in response to cholesterol suggests that these nuclear receptors are a possible therapeutic target, as these receptors tend to be inhibited in CRC and many other cancers (Gabitova *et al.*, 2013). Cellular receptors are particularly attractive targets for cancer therapy because they are activated by specific ligands and have distinct ligand binding domains that allow for specific and effective modulation (Lin and Gustafsson, 2015). Targeting nuclear receptors has been particularly effective in treating breast and prostate cancers, and advances in medicinal chemistry have facilitated the development of receptor-selective, full, partial, and inverse agonists for these receptors (Lin and Gustafsson, 2015). The structure of LXRs and their respective endogenous and synthetic ligands are well-established. Thus, our gap in knowledge is how these receptors exert their anti-proliferative effects in colon cancer. Establishing how LXR activity is limited will allow for more pre-clinical trials of LXR as an anti-cancer therapy target.

Focus of Thesis

KCNQ1, a gene which encodes for a voltage-gated ion channel, and *CFTR*, a gene which encodes for an ion channel which promotes chloride and bicarbonate secretion, have been identified by genetic studies as murine susceptibility genes for intestinal

tumorigenesis (Than *et al.*, 2016; Than *et al.*, 2013; Starr *et al.*, 2009). Mutation of *KCNQ1* is associated with several human disease syndromes including Jervell and Lange-Nielson syndrome, long QT syndrome, iron-deficiency anemia, gastric and duodenal hyperplasia, and enhanced risk for type-2 diabetes (Yasuda *et al.*, 2008). Similarly, mutation of *CFTR* is the causal genetic event for cystic fibrosis, a life-shortening disease that is the most common autosomal recessive disease in Caucasian populations.

Although *KCNQ1* and *CFTR* were identified as a susceptibility genes for colon cancer, their roles in disease development are largely unknown. Analysis of human CRC patient data show that patients with high KCNQ1 or high CFTR expression have better disease-free survival rates compared to patients with low expression of these genes (Than *et al.*, 2013; Than *et al.*, 2016). Thus, *KCNQ1* and *CFTR* have an implied role in colon cancer development, but functional characterization of this mechanism has not yet been established.

The goal of this thesis was to determine the tumor suppressive mechanisms of *KCNQ1* and *CFTR*. While developing our strategy for determining these mechanisms, we considered multiple experimental methods. Although many tissue culture systems have been established in efforts to investigate the pathology of colorectal cancer, no long-term culture system maintained basic crypt-villus physiology of the intestinal tissue (Sato *et al.*, 2009). Considering this, Sato *et al.* developed the intestinal organoid culture system. Intestinal organoids are comprised of isolated intestinal stem cells that recapitulate the self-renewal and differentiation capacity of the tissue of origin, thus modeling the stem

cell capacity of the tissue they are derived from. Five to six stem cells expressing the $Lgr5^{+}$ marker reside in the base of the crypt and can be isolated from the tissue and other differentiated cells by treatment with EDTA, vigorous washes, and differential centrifugation. These isolated stem cells can be grown in the absence of a non-epithelial cellular niche and self-organize into crypt-villus domains, in which all differentiated cell types are present, by undergoing multiple crypt-fission events (Sato *et al.*, 2009). While the organoids established by Sato utilize isolated stem cells, organoids can also be grown from isolated intestinal crypts, which is the protocol our lab utilizes. Organoids are grown in Matrigel, a 3D culture medium rich in laminin, to mimic the environment of the crypt base (Sato *et al.*, 2009). To provide the necessary growth requirements for the stem cells, Sato *et al.* established growth media supplemented with necessary factors to direct stem cell proliferation and differentiation. These advancements in culture systems allowed for a more simplified study of stem-cell-driven crypt villus biology (Sato *et al.*, 2009).

Previous studies by a former member of our lab, Dr. B.L.N Than, utilized intestinal organoids to determine the role of *KCNQ1* and *CFTR* in the stem cell compartment. Than *et al.* harvested intestinal organoids from the colons of littermate and gender matched *Kcnq1* $^{-/-}$ and *Cftr* $^{-/-}$ mice (2013 and 2016, respectively). Organoid growth was monitored and evaluated from days 2-5 post-plating (Than *et al.*, 2016). The data showed that loss of *Kcnq1* increased the number of colon organoids 3-fold. Than *et al.* found similar tumor suppressive effects in colon organoids derived from *Cftr* $^{-/-}$ mice, in which loss of *Cftr* enhanced colon organoid growth by 2.3-fold (Than *et al.* 2016).

These results suggest a potential role of *Kcnq1*and *Cftr* in regulating the intestinal stem cell compartment (Than *et al.*, 2016).

The specific focus of this thesis was to investigate *KCNQ1* and *CFTR* as colorectal cancer tumor suppressors by their role in regulating the stem cell compartment. To inform our experimental aims and hypotheses, we began by confirming the expression of KCNQ1 in crypts of the intestinal epithelium, where the stem cells reside. We then used Illumina high-throughput sequencing technology to analyze mRNA levels in organoids derived from *KCNQ1* WT and KO mice. This data allowed us to identify candidate biological pathways and processes that were altered due to loss of *KCNQ1*, and to design functional experiments to further confirm and explore these differences and their effects on the stem cell compartment. We used reverse-transcriptase quantitative PCR to analyze gene expression changes in $Kcnq1^{-/-}$ and $Cftr^{-/-}$ organoids in response to activation of specific biological pathways. From projects like this, it is our goal to characterize the tumor suppressive mechanism of *KCNQ1* and *CFTR* on the intestinal stem cell compartment. This understanding could lead to potential development of biomarkers for colorectal cancer as well as therapeutic targets.

Materials and Methods

Animal Models

C57BL/6-*Kcnq1* knockout mice were obtained from Dr. Karl Pfeifer (NIH). *Kcnq1* was inactivated in the germline of mice by insertion of a neomycin cassette into exon 2, the first common exon to all isoforms (Casimiro *et al.*, 2000). C57BL/6-*Cftrfl10* mice were obtained from Drs. Mitchell Drumm & Craig Hodges (CWRU). LoxP sites

flanking exon 10 of the *Cftr* gene were inserted, and *Cftr* was conditionally inactivated by Cre recombinase in the intestinal epithelium by control of the Villin promoter (Hodges *et al.*, 2008). All mice used in this study were housed per IACUC protocols and standards. Because CFTR knockout mice accumulate viscous mucus in their digestive organs, a commercially available osmotic laxative was added to the drinking water of these mice (Gavilyte-C, Gavis Pharmaceuticals, Somerset, NJ, USA). All animal experiments were conducted per protocol as approved by the University of Minnesota IACUC.

Organoid Culture: Harvesting and Plating

Littermate mice of approximately 8-14 weeks of age were selected in genotypic pairs (wildtype and knockout) for obtaining organoids. Mice were euthanized in a CO_2 chamber for 4-5 minutes, and the small intestine was removed and washed briefly in ice-cold 1X PBS. The small intestine was cut longitudinally along its entire length and scraped gently with a clean microscope slide to remove villi. The small intestine was then washed 2-3 times vigorously in petri dishes containing ice-cold 1X PBS. After washing, the small intestine was cut using a sterile razorblade into 2-3 mm pieces. These intestinal pieces were then transferred to a 50-mL conical tube containing approximately 10 ml ice-cold PBS. A plastic pipet tip was coated with FBS and used along with a Pipet-Aid to wash the intestinal pieces by resuspension in 10 ml ice-cold PBS. The pieces were brought into the tip and ejected out near the bottom of the conical tube, disturbing the intestinal pieces to remove cellular debris. This was repeated three times, and the pieces were allowed to settle before removing and discarding the supernatant. The amount of washes with 10 ml ice-cold PBS varies between each organoid prep. In general, intestinal

pieces were washed until the supernatant no longer appeared cloudy (8-10 washes for small intestine). After the last wash, intestinal pieces were resuspended in 25 ml ice-cold chelation buffer (1X PBS, 43.4 mM sucrose, 54.9 mM D-sorbitol, and mQ H_2O) and EDTA (2.5×10^{-3} M). The intestinal pieces were incubated in this chelation buffer and EDTA solution for 30 minutes on a rotating spinner at 4°C. After incubation, the supernatant containing EDTA was removed, and the intestinal pieces were washed with approximately 10 ml of ice-cold chelation buffer, pipetting the pieces up and down as described above. 10 µL of the supernatant was checked under the microscope for the presence of crypts after each new wash. Supernatants that contained crypts were pooled to a separate tube. The number of washes pooled varies between crypt preparations, but is generally between the second and tenth washes, and washes are pooled until no more crypts are seen in the supernatant.

The 50 mL conical tube with the pooled supernatants containing crypts was spun at 300 x g at 4°C for 5 minutes. The supernatant was removed, as the pellet contains the crypts. The pellet was resuspended in 10 ml ice-cold chelation buffer and filtered through a 70 µm cell strainer into a clean 50 mL conical tube. The pass-through was transferred to a 15 mL conical tube and spun at 200 x g for 4 minutes to pellet the crypts, the supernatant was discarded, and repeated 3-4 times. The pellet was resuspended in 10 ml ADF and a 20 µL aliquot was counted using a hemocytometer. The volume of the aliquots for plating was calculated by multiplying the number of crypts counted in a 20 µL aliquot by the total volume of ADF used to resuspend the crypt pellet in. Then, the number of crypts desired per well is divided by the concentration of crypts in the

suspsension to give the volume of crypts to and this resultant volume was aliquoted. The crypts resuspended in ADF were then aliquoted to 15 mL conical tubes and spun down to pellet. The pellet was resuspended in 200 µL Matrigel (growth factor reduced, phenol red free; BD Biosciences) and plated to 6 wells of a 24 well cell culture plate (approximately 1000 crypts per 30 µL of Matrigel per well). Once the Matrigel has solidified, 500 µL of ADF media (supplemented with Hepes, L-Glutamine, RSPO1, EGF, Noggin, B27, N2, N-Acetylcysteine, and primocin) was added to each well. Organoids were incubated at 37°C and 5% CO_2.

Organoid Culture: Passaging

Harvested organoids were passaged every six to seven days to maintain a consistent line. To each well of organoids, 500 µL Cell Recovery Solution (Corning, Cat. No. 354253) was added and plates were incubated at 4°C for one hour. The bottom of each well was gently scraped using a P1000 pipette, and the organoids suspended in Cell Recovery Solution were pooled together (per treatment and/or genotype) and diluted to approximately ten ml with ADF+Hepes+L-Glut. These pooled organoids were spun at 100 x g at 8°C for five minutes. The pellet is resuspended in approximately five ml of ADF+Hepes+L-Glut and the organoids were further disrupted by repeated pipetting up and down using a 2-mL plastic pipet tip with an additional unfiltered pipet tip stuck on the end. The disrupted organoids were spun again at 200 x g at 8°C for five minutes, and the resulting pellet was resuspended in 50 µL complete organoid media. Matrigel (100 µL) was added to this solution of media and organoids and the mix was plated evenly

across six wells of a 24-well plate. Organoids were plated and cultured per the previous section.

Organoid Culture: Treatment

Organoids were treated with either the LXR agonist GW3965 (Sigma, cat. no. G6295) or Thapsigargin, both at a final concentration of 1 µM. To prepare, the organoid growth media was changed the day prior to treatment. A 1 mM stock of GW3965 or Thapsigargin was diluted 1:4 in ADF. Two µL of this dilution was added to each well of organoids to be treated and left overnight before harvesting of RNA. As a control, an equal volume of 0.05% DMSO was added to each well.

MTT Assay

The cell viability of organoids derived from *Kcnq1* and *Cftr* WT and KO mice was measured using an MTT assay. This colorimetric assay measures the activity of cellular enzymes that convert MTT (3-(4,5-dimethylthiazol-2-yl)-2,5-diphenyltetrazolium bromide) to a purple formazan product by measuring the absorbance of the solution. The amount of signal generated is dependent on the concentration of MTT, the length of the incubation period, the number of viable cells, and metabolic activity of the cells being analyzed (Riss *et al.*, 2013). Organoids were plated in a 96-well plate for the MTT assay. To recover the organoids for passaging, the Matrigel was mechanically disrupted by vigorous pipetting, washed with ADF, and centrifuged at high speeds (800-1,000 rpm for four minutes). The organoids were pooled together and then serially diluted from the

pooled sample, which served as the undiluted “stock.” The tubes were prepared as follows: the “100” sample contained 2 mL “stock”; the “75” sample contained 1.5 mL “stock” and 0.5 mL ADF; the “50” sample contained 1 mL “stock” and 1 mL ADF; the “25” sample contained 0.5 mL “stock” and 1.5 mL ADF. These diluted tubes were spun at 800-1,000 rpm for an additional four minutes to pellet the organoids. The pellet was resuspended in 100 µL Matrigel and plated to a pre-warmed 96-well plate, approximately one drop of the Matrigel and organoid suspension per well. An additional row of wells were plated with Matrigel and no organoids as a control. Once the Matrigel had solidified, 100 µL complete crypt culture media was added to each well, and the 96-well plate was incubated at 37°C and 5% CO_2.

The organoids grew in the 96-well plate for three days before the addition of the MTT reagent at 500 µg/mL per well (Roche, Version 18, cat. no. 11-465-007-001). The addition of MTT was followed by an incubation period of two to three hours at 37°C and 5% CO_2. To solubilize the Matrigel, the media and MTT was aspirated using a Pasteur pipet and 20 µL SDS was added per well and incubated for an additional two hours at 37°C and 5% CO_2. To solubilize reduced MTT, 100 µL DMSO was added per well followed by a one hour incubation at 37°C. The OD was measured on a microplate reader at 562nM. Sample absorbencies were normalized using the absorbencies measured from the control wells. Normalized measured absorbencies from WT and KO wells were compared by their respective dilution (100, 75, 50, and 25) to determine differences in the MTT signal between samples.

RNA Isolation

RNA was isolated from intestinal organoids approximately 4 days post-plating. The Qiagen RNEasy Mini Kit (Cat. No. 74104) was used per the manufacturer's protocol, with the following modifications. Media was removed from the organoids using a sterile glass pipet attached to a vacuum. Matrigel was dissolved by adding 500 µL Cell Recovery Solution (Corning, Cat. No. 354253) and incubated at 4°C for one hour. Once dissolved, three to six wells were pooled in 15 mL conical tubes and filled with ADF, then spun at 200 x g for five minutes at 4°C. The supernatant was discarded and samples were pooled together, resuspended in approximately 15 ml ADF, and spun again at 200 x g for 5 minutes at 4°C. After the samples were pooled, the supernatant was removed and the pellet was resuspended in 175 µL RLN (supplemented with RNAsin and 1M DTT) and incubated on ice for five minutes. The samples were spun at 300 x g for two minutes at 4°C, and the supernatant was transferred to an RNA-free Eppendorf tube. The rest of the procedure followed the manufacturer's protocol (Qiagen RNEasy Mini Kit, Cat. No. 74104). The final concentration of RNA was measured on a NanoDrop in ng/µL.

Immunohistochemistry

Expression and localization of *KCNQ1* was analyzed by immunohistochemistry of mouse tissue. Small intestine and colon were harvested from littermate mice and washed in PBS to remove excess fecal matter. The tissue was sprayed with 70% ethanol and was fixed overnight in formalin. Fixed tissues were dehydrated by an automated Tissue-Tek VIP processor and embedded in paraffin blocks using the Leica EG1160.

Paraffin embedded tissues were sectioned at five microns with a Reichert-Jung 2030 microtome and were mounted to charged microscope slides. The mounted slides were dried in a 60°C oven for 30 minutes and subsequently deparaffinized in xylene, followed by a rehydration process with a series of ethanol washes. Antigen retrieval was performed with rodent decloaker in an 85°C water bath for 40 minutes. The primary antibody KCNQ1 (H-130, Santa Cruz cat. no. sc-20816) was used at a concentration of 1:150 and incubated overnight at 4°C. Bound antibodies were detected using goat anti-rabbit IgG Alexa Fluor 568 (1:500, Fisher Scientific cat. no. A11036) and Prolong Diamond Antifade DAPI (Life Technologies, cat. no. P36966). DAB Chromogen (Biocare Medical LLC cat. no. DB801R) was also used to detect bound antibodies. Image acquisition was performed using a Zeiss LZM710 laser scanning confocal microscope.

Illumina Next-Generation RNA Sequencing

RNA was isolated from *CFTR* and *KCNQ1* WT and KO organoids as previously described. For RNA quality control, the protein concentration was determined using a Nanodrop and one µg of each sample was sent to the University of Minnesota Biomedical Genomics Center (Minneapolis, MN) to analyze distinct 28s and 18s bands. These ribosomal RNA bands are a visual way to analyze the quality of total RNA, and crisp bands indicate intact RNA, as well as intact mRNA, which cannot be visualized with electrophoresis. 2,000 ng of RNA per well (concentration of 100 ng/µL) of three paired samples (WT and KO) per genotype (*CFTR* and *KCNQ1*) were sent to the University of Minnesota Biomedical Genomics Center (Minneapolis, MN) for Illumina

Next-Generation RNA sequencing following the UMGC's submission instructions. Illumina Next-Generation RNA sequencing is a high-throughput sequencing system that produces between 300 million - 2 billion sequence reads per run of lengths between 50-500 bp. Next-Generation RNA sequencing uses mRNA fragments to produce cDNA templates which undergo short-read sequencing. These sequences are then aligned to a reference genome sequence to determine relative expression levels of genes in the experimental sample. We used the high-throughput raw expression data we obtained from this analysis as a dataset for Gene Set Enrichment Analysis (Broad Institute) to determine gene sets that were enriched (comparatively high expression) or depleted (comparatively low expression) between the two sets of organoids, *KCNQ1* or *CFTR* WT and KO.

Reverse-Transcriptase Quantitative Polymerase Chain Reaction

Target gene expression was analyzed and compared between *KCNQ1* and *CFTR* WT and KO organoids by reverse-transcriptase quantitative polymerase chain reaction (RT-qPCR). RT-qPCR monitors the amplification of a targeted DNA molecule during the polymerase chain reaction in real time using non-specific fluorescent dyes that incorporate into double-stranded DNA. Absolute quantification can be used to quantify the copy number of specific nucleic acids in a sample by comparison with DNA standards using a calibration curve. Gene standards were created by first reverse-transcribing 1.5 µg mouse colon RNA using Qiagen Omniscript RT Kit (cat. no. 205113) and gene-specific primers. The standard cDNA was amplified using Qiagen HotStarTaq Master Mix Kit (cat. no.203443) and purified using the Qiagen MinElute PCR

Purification Kit (cat. no. 28004). 0.5-1.5 µg RNA isolated from *CFTR* and *KCNQ1* WT and KO organoids (as previously described) was reverse-transcribed to cDNA using Qiagen Omniscript RT Kit (cat. no. 205113) and random 9 primers. The organoid sample cDNA was diluted 1:10 for analysis of specific target genes and 1:100 for analysis of 18S standard genes. 18S standard curves were amplified from a dilution range of $1e^8$ copies/µL to $1e^3$ copies/µL. All samples and standards were plated in duplicate on a 96-well plate using a Roche Light Cycler480 Real-Time PCR Instrument with the following cycle parameters: pre-incubation- one cycle, 95°C for five minutes; amplification- 45 cycles, 95°C for five seconds, 60°C for five seconds, and 72°C for ten seconds; melt curve- one cycle, 95°C for five seconds, 65°C for one minute, and 97°C continuous; and cooling- one cycle at 40°C for 30 seconds. To perform concentration analysis, the LightCycler 480 Real-Time PCR Instrument was used. Because both quantity and quality of mRNA may vary from sample to sample, an internal control was used for analysis. 18S is a ribosomal subunit expected to be expressed ubiquitously and relatively uniformly across samples. Thus, it is an accurate way to normalize target gene expression between experimental samples to controls and correct sample variability. Standard curves were calculated for both 18S and target genes using mRNA samples of known concentrations. These standard curves serve as a reference standard for extrapolating quantitative information for sample mRNA targets of unknown concentration.

Gene Set Enrichment Analyses

Transcriptomic analysis was performed using Gene Set Enrichment Analysis (GSEA) software from the Broad Institute. GSEA is a statistical method to identify groups of genes (gene sets) that are significantly enriched or depleted in a given set of gene expression data (datasets). This analysis provides a functional profile of the experimental dataset to better evaluate the underlying biological processes that may be altered due to phenotypic differences between the samples. The datasets used for analysis were from previously published studies of primary human tumor samples analyzed by Affymetrix Human Genome U133 Plus 2.0 Array and can be found under GEO accession numbers: GSE33113, GSE14333, and GSE13294. The datasets were sorted continuously for *KCNQ1* low to high expression or sorted continuously for *CFTR* low to high expression and the Pearson correlation coefficient was the statistical analysis used. The hallmark signature gene set was found in the molecular signatures database. The genes in this gene set were determined based on overlaps in other molecular signatures database gene sets and retaining genes that display coordinate expression. The parameters of the GSEA for all three dataset analyses were weighted enrichment statistic and Pearson correlation coefficient as the metric for ranking genes. The top four gene sets that were enriched in all three tumor datasets were identified.

Results

Kcnq1 is expressed at the base of the colonic crypt

The goal of this study was to evaluate our working model of KCNQ1 tumor suppression by utilizing gene expression analysis, both targeted and global, as well as

functional assays. We hypothesized that the loss of *KCNQ1* causes oncogenic changes to the stem cell compartment of the intestinal epithelium. To begin, we needed to confirm Kcnq1 is expressed in the stem cell compartment of murine colon. Immunohistochemical analysis for the protein showed the highest expression near the base of the crypt (Figure 1). The signal diffuses as it progresses up the crypt, and is virtually absent near the top of the crypt. This data confirms that Kcnq1 is expressed in the base of the crypt compartment of murine colonic tissue, where the stem cells are known to reside. A similar immunohistochemical analysis was published by Preston *et al.* (2011) and was used as a reference for developing this protocol. These results confirm the results of Preston *et al.* (2011).

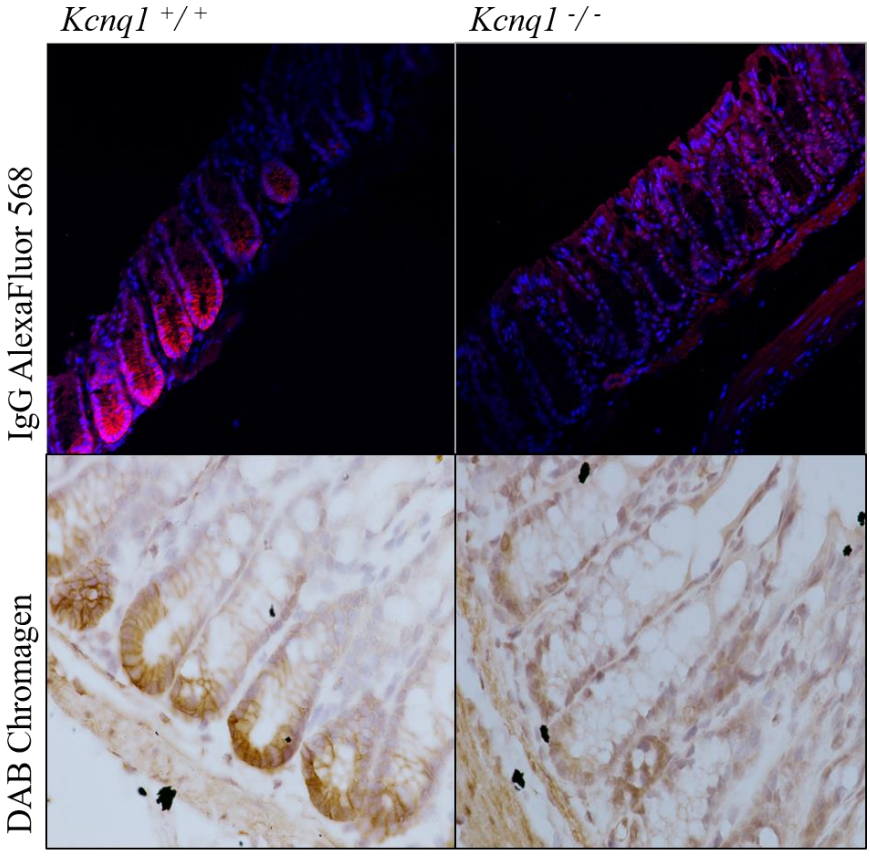

Figure 1. *Kcnq1 is expressed in the base of the crypt. Kcnq1* staining on representative colonic sections of animals of indicated genotypes. Magnification 20X.

MTT Analysis of Organoids

Organoids harvested from *Kcnq1* KO and WT mice as well as *Cftr* WT and KO mice were analyzed for differences in cell viability using the MTT assay. These ratios allow for comparison of the KO MTT signal at all four dilutions (100, 75, 50, 25) to the WT 100 MTT signal as the baseline of 1. Thus, any increase or decrease of the MTT signal in the KO organoids is in comparison to the WT 100 MTT signal value. The organoids derived from *Kcnq1* KO mice have a slightly higher MTT signal at all four relative dilutions, although a two-way ANOVA analysis determined this difference is not statistically significant at $p \leq 0.05$ (Figure 2a). Similarly, organoids derived from *Cftr* KO mice have a slightly higher MTT signal at all four relative dilutions (Figure 2b). Analysis of these values with a two-way ANOVA determined this difference in MTT signal is also not statistically significant ($p \leq 0.05$).

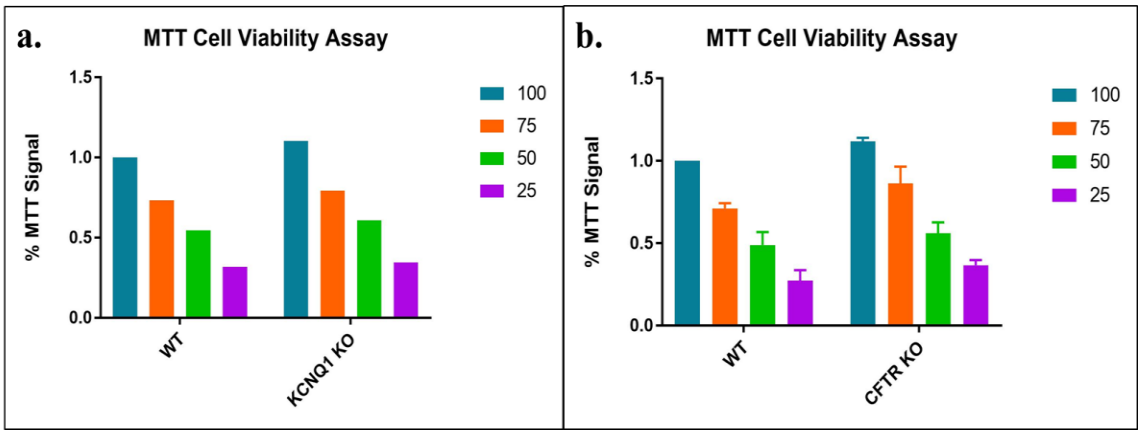

Figure 2. *MTT Cell Viability Assay of Organoids.* **a.** *Kcnq1* KO organoids have a slightly higher MTT signal compared to WT organoids. **b.** *Cftr* KO organoids have a slightly higher MTT signal compared to WT organoids.

Organoid RNA Quality Assessment

Once we had confirmed the expression of Kcnq1 in the stem cell compartment of the intestinal crypt, we proceeded to organoid studies. Organoid RNA was harvested from pairs of *Kcnq1* $^{+/+}$ and *Kcnq1* $^{-/-}$ littermate mice for Illumina Next-Generation RNA Sequencing by the University of Minnesota Genomic Center after analysis of RNA quality. I harvested and cultured the organoids with help from Kyle Anderson, and Kyle Anderson isolated organoid RNA and also organized and prepared the RNA samples for sequencing. Figure 3 shows two distinct ribosomal RNA bands at 18s and 28s, which indicate total RNA derived from organoid samples was overall intact.

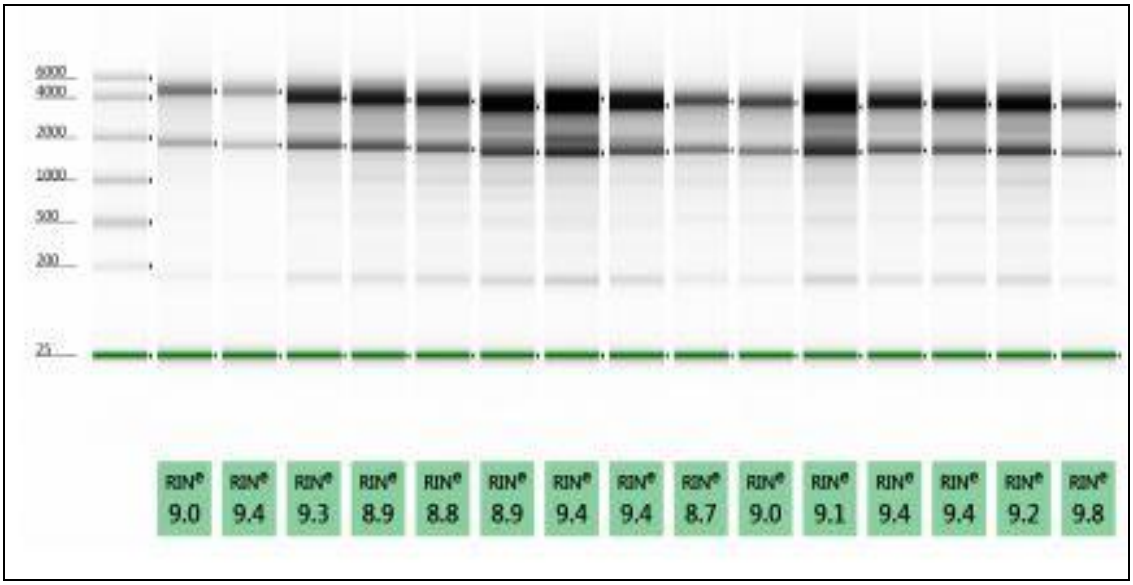

Figure 3. *Organoid RNA quality assessment.* All organoid RNA pairs passed quality control analysis and display two solid bands representing 18s (2,000 bp) and 28s (4,000-6,000 bp) ribosomal RNA.

Illumina Next-Generation RNA Sequencing of Organoid RNA

Illumina Next-Generation RNA Sequencing was performed on *Kcnq1* $^{+/+}$ and *Kcnq1* $^{-/-}$ organoid RNA by the University of Minnesota Genomics Center. Three *Kcnq1* WT and KO organoid RNA pairs were analyzed. Hi-Seq 2500 High-Output was run on these samples and detected over 21,000 different transcripts.

Gene Set Enrichment Analysis of Organoid RNA Sequencing Data

RNA expression data from three *Kcnq1* $^{+/+}$ and $^{-/-}$ littermate paired mice was analyzed using GSEA software from the Broad Institute. GSEA is a useful tool for interpreting genome-wide expression profiles because it utilizes gene sets, or groups of genes that share common biological function (Subramanian *et al.*, 2005). Based on previous GSEA analyses of this dataset that found the unfolded protein response (UPR) was enriched in the *Kcnq1* KO organoids, we then further analyzed this enrichment. The UPR gene set used in this analysis was previously published by Han *et al.* (2009). GSEA determined upregulation of the UPR gene set in *Kcnq1* WT organoids and downregulation of the UPR gene set in *Kcnq1* KO organoids by comparing these as two distinct phenotypes (Figure 4). Although one representative enrichment plot is shown here, all unfolded protein response gene sets ran also showed similar enrichment in the *Kcnq1* KO phenotype. This specific gene set, published in Han *et al.* 2009, includes genes involved in the IRE1α arm of the UPR that were upregulated 2-fold upon activation of the UPR. This data suggests that the loss of *Kcnq1* affects either the activation of the unfolded protein response in organoids (by altering expression of genes directly involved in the UPR) or affects the response of these organoids to activation of the UPR via downstream pathways that result because of UPR activation.

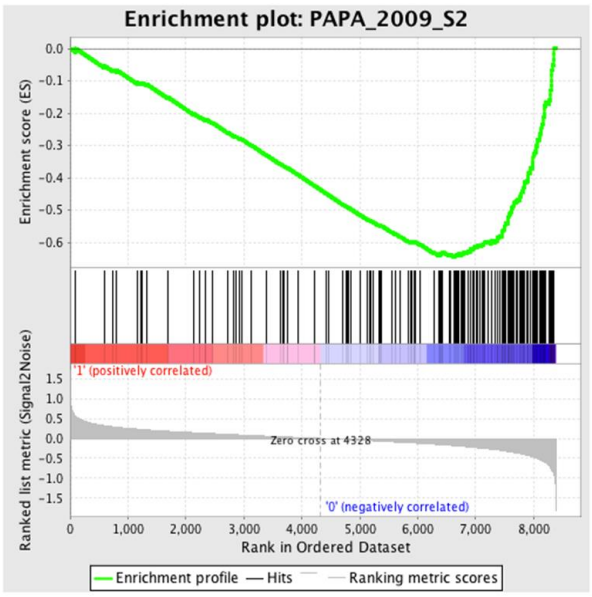

Figure 4. *UPR Gene Set Enrichment Plot.* The unfolded protein response gene set is enriched in the *Kcnq1* WT organoids compared to the *Kcnq1* KO organoids. The enrichment plot shows a profile of the running enrichment score and positions of gene set members on the rank ordered list.

Gene Set Enrichment Analysis of Primary Tumor RNA Sequencing Data

RNA expression data (HG-U133_Plus_2 Affymetrix Human Genome U133 Plus 2.0 Array) from three public GEO Datasets was analyzed using GSEA. The mRNA used in each dataset was derived from the following samples: dataset GSE33113 consisted of primary tumor resections from 90 Stage II CRC patients and matching normal colon tissue from 6 of these patients; dataset GSE14333 consisted of 290 primary colorectal tumor samples; dataset GSE13294 consisted of 155 primary colorectal tumor samples. The datasets were sorted continuously, either as *KCNQ1* low to high expression, or *CFTR* low to high expression. The hallmarks of cancer gene set (Molecular Signatures Database (MSigDB), Broad Institute, h.all.v6.0.symbols) was run against these datasets, and the negative Pearson correlation coefficient statistical test was used to determine the top four gene sets enriched in the knockout phenotype in all three datasets. The hallmarks of

cancer gene set is a collection of gene sets that summarize and represent the biological state of cancer and display coherent expression. These gene sets were generated by a computational methodology based on identifying overlaps between gene sets in other MSigDB collections and retaining genes that display coordinate expression (Subramanian *et al.*, 2005).

Gene Set Enrichment Analysis of Tumor Data- KCNQ1

To gain insight into the biological pathways affected by the loss of *KCNQ1* in humans, we used GSEA to determine gene sets that were enriched or depleted in human tumor mRNA. The three primary tumor datasets were sorted continuously for low to high *KCNQ1* expression. GSEA was performed on these datasets for the hallmarks of cancer gene set. Table 1 shows the top four gene sets that were enriched in the *KCNQ1* low phenotype in all three datasets. The top gene sets were selected by the false discovery rate (FDR) cutoff of 0.25. The epithelial mesenchymal transition gene set was enriched at a statistically significant level in the *KCNQ1* low phenotype of all three tumor datasets. The inflammatory response gene set was enriched at a statistically significant level in the *KCNQ1* low phenotype of two tumor datasets (14333 and 13294), although it was not found to be enriched in the tumor dataset 33113. The allograft rejection and interferon gamma response gene sets were enriched at a statistically significant level in all three tumor datasets.

	Epithelial Mesenchymal Transition		Inflammatory Response		Allograft Rejection		Interferon Gamma Response	
	FDR	NES	FDR	NES	FDR	NES	FDR	NES
33113 Primary tumor resections, Stage II	0.075	-1.112	---	---	0	-1.334	0	-1.279
14333 Primary colorectal tumor samples	0	-2.336	0	-1.910	0.0253	-1.737	0.0682	-1.466
13294 Primary colorectal tumor samples	0.026	-1.557	0	-2.212	0	-2.369	0	-2.368

Table 1. *Gene sets enriched in the KCNQ1 low expressing tumor samples.* False discovery rate (FDR) and the normalized enrichment score (NES) are shown for each dataset and gene set.

Gene Set Enrichment Analysis of Kcnq1 $^{+/+}$ and $^{-/-}$ Organoids

We performed GSEA on *Kcnq1* $^{+/+}$ and $^{-/-}$ organoid mRNA expression data to determine which gene sets were enriched or depleted due to loss of *Kcnq1*. The enriched or depleted gene sets informed us of what associated biological pathways may be affected by the loss of *Kcnq1*, as well as whether these pathways affect the stem cell compartment of the tissue. By comparing the enriched gene sets to the gene sets determined as enriched in the *KCNQ1* low tumor data, we can compare tumor tissue gene expression changes and stem cell compartment gene expression changes due to loss of *Kcnq1*. This analysis was performed differently from the previous one (Table 1), as the phenotype was not continuous, but was set as two distinct phenotypes (*Kcnq1* $^{+/+}$ and $^{-/-}$).

Table 2 shows the top four enriched gene sets in the *Kcnq1* $^{-/-}$ organoid phenotype. The inflammatory response and epithelial mesenchymal transition gene sets were enriched in *Kcnq1* $^{-/-}$ organoids at a statistically significant level (FDR of 0.004 and 0.020, respectively). These gene sets were also found to be enriched in the *KCNQ1* low expressing tumor sample phenotype. The cholesterol homeostasis and IL6 JAK-STAT3 signaling pathway gene sets were also enriched at a statistically significant level (FDR of 0.027 and 0.027, respectively), but were not found to be enriched in the tumor datasets.

Generally, these enriched gene sets are interesting and important because of the well-researched and established role of inflammation in cancer development and progression. It is also important to note than some of the enriched processes in tumors are also enriched in organoids, supporting intestinal organoids as a sufficient experimental model.

	Inflammatory Response		Cholesterol Homeostasis		Epithelial Mesenchymal Transition		IL-6 JAK-STAT3 Signaling Pathway	
	FDR	NES	FDR	NES	FDR	NES	FDR	NES
***Kcnq1*$^{-/-}$ organoids**	0.004	-1.94	0.027	-1.73	0.020	-1.71	0.027	-1.64

Table 2. *Gene sets enriched in the Kcnq1* $^{-/-}$ *organoids.* False discovery rate (FDR) and the normalized enrichment score (NES) are shown for each gene set.

Gene Set Enrichment Analysis of Tumor Data- CFTR

To gain insight to the biological pathways affected by the loss of *CFTR* in humans, we used GSEA to determine gene sets that were enriched or depleted in human tumor mRNA. The three primary tumor datasets were sorted continuously for low to high

CFTR expression. GSEA was performed on these datasets for the hallmarks of cancer gene set. Table 3 shows the top four gene sets that were enriched in the *CFTR* low phenotype in all three datasets. The gene sets were considered significant by the false discovery rate cutoff of 0.25. The epithelial mesenchymal transition gene set was enriched in the *CFTR* low phenotype of all three tumor datasets, but not at a statistically significant level. The inflammatory response gene set was enriched at a statistically significant level in the *CFTR* low phenotype of two tumor datasets (33113 and 13294), although it was not found to be enriched in the tumor dataset 14333. The tumor necrosis factor (TNF) signaling via NF-κB gene set was enriched in the *CFTR* low phenotype of two of the tumor datasets (14333 and 13294) but was not significantly enriched in 33113. The angiogenesis gene set was enriched at a statistically significant level in all three tumor datasets.

	Epithelial Mesenchymal Transition		Inflammatory Response		TNF Signaling via NF-κB		Angiogenesis	
	FDR	NES	FDR	NES	FDR	NES	FDR	NES
33113 Primary tumor resections, Stage II	0.592	-1.254	0.217	-1.204	0.383	-1.220	0.256	-1.219
14333 Primary colorectal tumor samples	0.441	-1.641	0.264	-1.535	0.196	-1.625	0.225	-1.508
13294 Primary colorectal tumor samples	0.286	-1.293	0.007	-1.969	0.040	-1.784	0.234	-1.367

Table 3. *Gene sets enriched in the CFTR low expressing tumor samples.* False discovery rate (FDR) and the normalized enrichment score (NES) are shown for each dataset and gene set.

RT-qPCR Analysis of Kcnq1 $^{+/+}$ and Kcnq1 $^{-/-}$ Organoids

Organoids were harvested and cultured from pairs of *Kcnq1* $^{+/+}$ and *Kcnq1* $^{-/-}$ mice, and mRNA was isolated from these cultures. RT-qPCR was performed on this RNA to analyze gene expression changes of target genes in the WT and KO organoids. Previous GSEA data showed that in *Kcnq1*-deficient tissue expression of the unfolded protein response (UPR) gene set is depleted. To investigate this further, we treated one pair of *Kcnq1* $^{+/+}$ and *Kcnq1* $^{-/-}$ organoids with Thapsigargin, an inducer of the UPR. RNA was isolated from these organoids for analysis by RT-qPCR. The target gene activating transcription factor 4 (*Atf4*) was analyzed in both treated and untreated *Kcnq1* $^{+/+}$ and *Kcnq1* $^{-/-}$ organoids (Figure 5). *Atf4* is a regulatory element that increases protein folding, transport, and ER-associated protein degradation, while attenuating protein synthesis (Wang and Kaufman, 2014). The basal expression level of *Atf4* in *Kcnq1* $^{-/-}$ organoids is slightly higher than the basal expression of this gene in *Kcnq1* $^{+/+}$ organoids. However, the expression level of *Atf4* is slightly lower in *Kcnq1* $^{-/-}$ organoids after treatment with Thapsigargin and induction of the unfolded protein response. An unpaired t-test was run to analyze the statistical significance of these data, as well as the entirety of the RT-qPCR data in this thesis (unpaired t-test, all samples assumed to be sampled from populations with the same standard deviation, $\alpha=0.05$ for multiple comparisons using the Holm-Sidak method). The difference between the control expression levels is not statistically significant at $p \leq 0.05$ ($p=0.0781$). However, the WT organoids express *Atf4* in response

to treatment with Thapsigargin at a significantly higher amount than in *Kcnq1* $^{-/-}$ organoids after treatment with Thapsigargin at $p \leq 0.05$ (p=0.0056). This data suggests loss of *Kcnq1* in organoids has an effect on the expression of *Atf4* in response to induction of the unfolded protein response, as it is clear the organoids both respond to treatment. To confirm these results, more replicates should be tested.

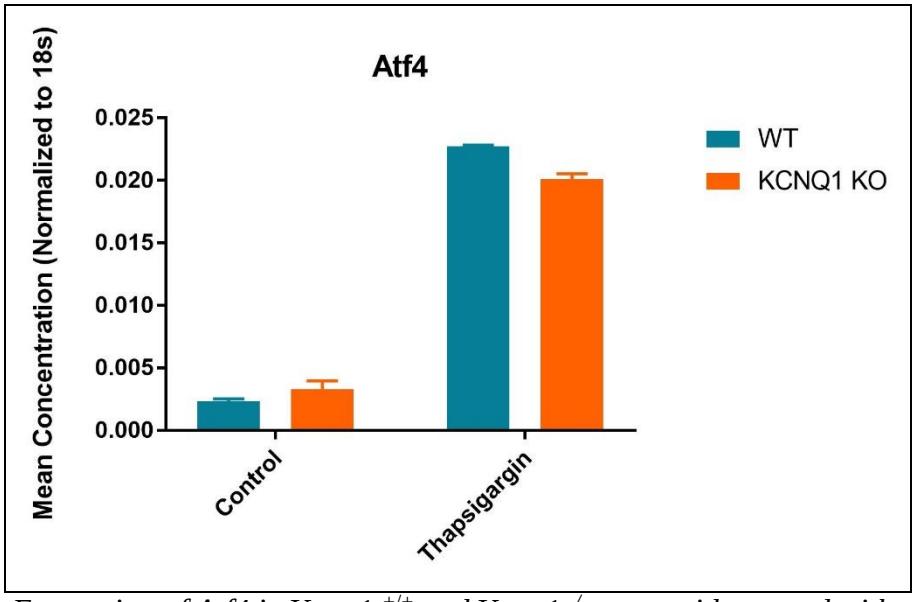

Figure 5. *Expression of Atf4 in* Kcnq1 $^{+/+}$ *and* Kcnq1 $^{-/-}$ *organoids treated with Thapsigargin*. The basal level of Atf4 expression is slightly increased in *Kcnq1* $^{-/-}$ organoids compared to *Kcnq1* $^{+/+}$ organoids. *Kcnq1* $^{-/-}$ have a decreased response to UPR induction by treatment with Thapsigargin compared to *Kcnq1* $^{+/+}$ organoids. The standard error for technical replicates is shown by the error bars.

In addition, expression of heat shock protein A member 5 (*Hspa5*) was analyzed in *Kcnq1* $^{+/+}$ and *Kcnq1* $^{-/-}$ organoids treated with Thapsigargin as well as in untreated controls (Figure 6). *Hspa5* encodes the protein endoplasmic reticulum luminal glucose-regulated protein 78 (GRP78), which functions as an unfolded protein response (UPR) signaling regulator by binding to and maintaining ER stress sensors PERK, ATF6, and IRE1. The basal expression of *Hspa5* in both the *Kcnq1* $^{+/+}$ and *Kcnq1* $^{-/-}$ organoids is

quite low, and although the *Kcnq1* $^{-/-}$ organoids have a slightly higher expression level, this difference is not significant $p \leq 0.05$ ($p=0.3947$). After treatment with Thapsigargin, the expression of *Hspa5* drastically increases in both the *Kcnq1* $^{+/+}$ and *Kcnq1* $^{-/-}$ organoids. However, like the expression of *Atf4*, the expression level of *Hspa5* is significantly lower in *Kcnq1* $^{-/-}$ organoids after induction of the UPR at $p \leq 0.05$ ($p=0.0362$). This data suggests loss of *Kcnq1* in organoids has an effect either on the expression of *Hspa5* in response to induction of the unfolded protein response, or on the response of organoids to this treatment. This experiment was performed using only one biological replicate. More replicates must be obtained and evaluated to confirm or refute these results.

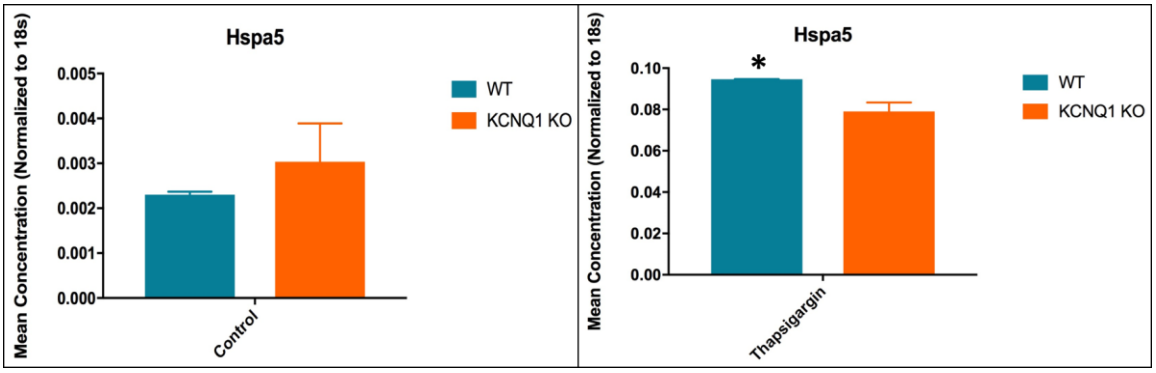

Figure 6. *Expression of Hspa5 in* Kcnq1 $^{+/+}$ *and* Kcnq1 $^{-/-}$ *organoids treated with Thapsigargin*. The basal level of *Hspa5* expression is slightly increased in *Kcnq1* $^{-/-}$ organoids compared to *Kcnq1* $^{+/+}$ organoids. *Kcnq1* $^{-/-}$ organoids have a decreased response to UPR induction by treatment with Thapsigargin compared to *Kcnq1* $^{+/+}$ organoids. The standard error for technical replicates is shown by the error bars.

In addition to analyzing expression of UPR target genes in *Kcnq1* $^{+/+}$ and *Kcnq1* $^{-/-}$ organoids treated with Thapsigargin, we analyzed two intestinal stem cell signature genes, Achaete-Scute Family BHLH Transcription Factor 2 (*Ascl2*) and Leucine-rich repeat-containing G-protein coupled receptor 5 (*Lgr5*). Previous data show induction of

the UPR by Thapsigargin suppresses the expression of stem cell signature genes and UPR genes are highly expressed in differentiated cells, such as transit amplifying cells (Heijmans *et al.*, 2013).

Ascl2 is an intestinal stem cell marker gene that encodes a transcription factor whose related pathways include embryonic and pluripotent stem cell differentiation pathways and lineage specific markers. Expression of *Ascl2* in *Kcnq1* $^{+/+}$ and $^{-/-}$ organoids treated with Thapsigargin was analyzed using RT-qPCR (Figure 7). The data show basal expression of *Ascl2* is slightly higher in *Kcnq1* $^{-/-}$ organoids compared to *Kcnq1* $^{+/+}$ organoids, but this is not a significant difference at $p \leq 0.05$ ($p=0.0529$). The expression level of *Ascl2* drastically decreased after treatment with Thapsigargin in both *Kcnq1* $^{+/+}$ and *Kcnq1* $^{-/-}$ organoids, however, the *Kcnq1* $^{-/-}$ organoids express *Ascl2* at a lower level after induction of the UPR compared to *Kcnq1* $^{+/+}$ organoids, but this is not a significant difference at $p \leq 0.05$ ($p=0.0723$). These data suggest that loss of Kcnq1 in intestinal organoids affects the expression of *Ascl2* in the basal state as well as the expression of *Ascl2* in response to treatment with Thapsigargin and induction of the UPR. These results were obtained from one biological replicate. More replicates and experiments are needed to confirm or refute these results.

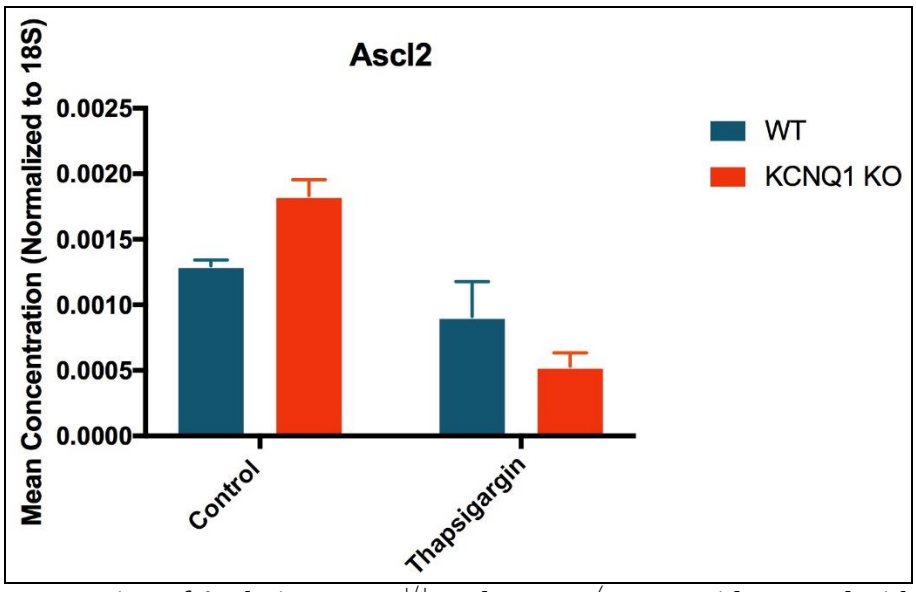

Figure 7. *Expression of Ascl2 in* Kcnq1 $^{+/+}$ *and* Kcnq1 $^{-/-}$ *organoids treated with Thapsigargin.* The basal level of *Ascl2* expression is slightly increased in *Kcnq1* $^{-/-}$ organoids compared to *Kcnq1* $^{+/+}$ organoids. *Kcnq1* $^{-/-}$ organoids have a decreased response to UPR induction by treatment with Thapsigargin compared to *Kcnq1* $^{+/+}$ organoids. The standard error for technical replicates is shown by the error bars.

The expression levels of intestinal stem cell marker gene *Lgr5* showed a similar trend (Figure 8). The basal expression level of *Lgr5* was higher in *Kcnq1* $^{-/-}$ organoids compared to *Kcnq1* $^{+/+}$ organoids, and according to a t-test, this difference is significantly different at $p \leq 0.05$ ($p=0.0347$). After treatment with Thapsigargin, the expression of Lgr5 in both *Kcnq1* $^{-/-}$ and *Kcnq1* $^{+/+}$ organoids drastically decreases, but the difference between *Kcnq1* $^{-/-}$ and *Kcnq1* $^{+/+}$ organoids is not significant at $p \leq 0.05$ ($p=0.5577$). This data supports previous studies that show induction of the UPR suppresses the expression of intestinal stem cell marker genes, but we cannot conclude there is a difference in this suppression due to loss of *Kcnq1*. This experiment was performed using only one biological replicate. More replicates must be obtained and evaluated to confirm or refute these results.

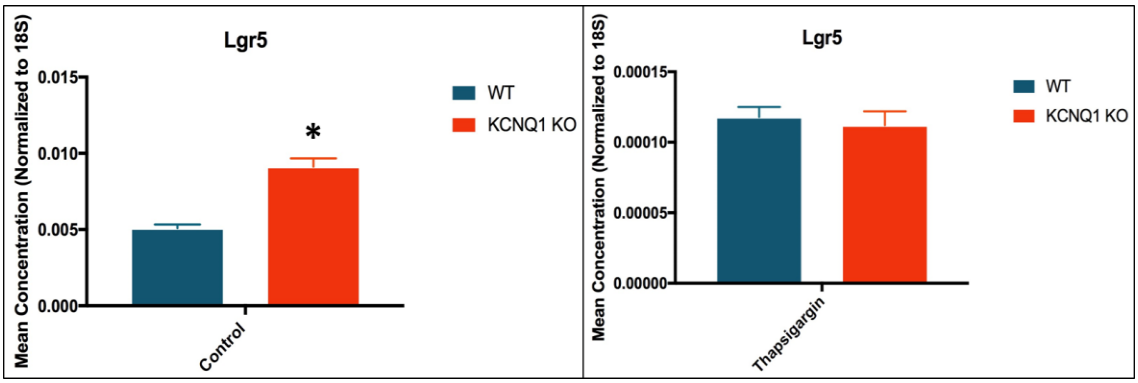

Figure 8. *Expression of Lgr5 in* Kcnq1 $^{+/+}$ *and* Kcnq1 $^{-/-}$ *organoids treated with Thapsigargin*. The basal level of Lgr5 expression is slightly increased in *Kcnq1* $^{-/-}$ organoids compared to *Kcnq1* $^{+/+}$ organoids. The expression of Lgr5 in response to UPR induction by treatment with Thapsigargin is virtually absent in both *Kcnq1* $^{+/+}$ and *Kcnq1* $^{-/-}$ organoids. The standard error for technical replicates are shown by the error bars.

RT-qPCR Analysis of Cftr$^{+/+}$ *and Cftr* $^{-/-}$ *Organoids*

Reverse-transcriptase quantitative polymerase chain reaction (RT-qPCR) was used to analyze differences in gene expression between organoids derived from the intestinal tissue of littermate mice, whose genotype was either wildtype or deficient for *Cftr*. Ingenuity Pathway Analysis (IPA) of *CFTR* normal and deficient tissue performed by previous members of our lab revealed that the LXR/RXR pathway was inhibited in *CFTR*-deficient tissue compared to normal tissue. To further analyze this inhibition, we treated one pair of *Cftr*$^{+/+}$ and *Cftr* $^{-/-}$ organoids with the LXR agonist GW3965 and analyzed gene expression of genes associated with this pathway, stearoyl-CoA desaturase-1 (*Scd1*) and aldehyde dehydrogenase 1 family, member A1 (*Aldh1a1*).

Scd1 encodes an enzyme that produces monounsaturated fatty acids, which serve as substrates for various kinds of lipids involved in a multitude of biological processes. The basal expression level of *Scd1* is quite low in both *Cftr*$^{+/+}$ and *Cftr* $^{-/-}$ organoids, but significantly higher in *Cftr*$^{+/+}$ organoids at $p \leq 0.05$ ($p=0.0086$, Figure 9). After treatment

with LXR agonist GW3965, expression of *Scd1*increases in both *Cftr*$^{+/+}$ and *Cftr* $^{-/-}$ organoids, however, the expression level is significantly higher in *Cftr*$^{+/+}$ organoids at $p \leq 0.05$ (p=0.0125). What should be noted about this data is that the ratio of the change in expression of *Scd1* before and after treatment with GW3965 is greater in *Cftr*$^{+/+}$ organoids compared to *Cftr* $^{-/-}$ organoids. This suggests that loss of *Cftr* may have an effect on the expression of *Scd1* in response to treatment with LXR agonist in organoids. Only two biological replicates were evaluated in this experiment. More replicates are needed to confirm or refute this result.

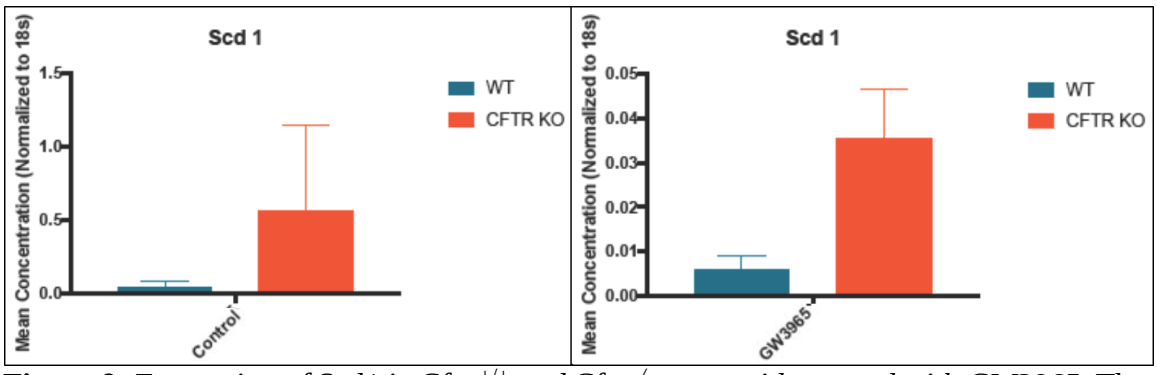

Figure 9. *Expression of Scd1 in* Cftr $^{+/+}$ *and* Cftr $^{-/-}$ *organoids treated with GW3965*. The basal level of *Scd1* expression is increased in *Cftr* $^{+/+}$ organoids compared to *Cftr* $^{-/-}$ organoids. The expression of *Scd1* in response to LXR/RXR pathway agonist GW3965 is stronger in *Cftr* $^{+/+}$ organoids than *Cftr* $^{-/-}$ organoids. The standard error for technical replicates are shown by the error bars.

Another gene we tested for differences in expression levels between *Cftr* $^{+/+}$ and *Cftr* $^{-/-}$ organoids is *Aldh1a1*. *Aldh1a1* is the second major enzyme in the oxidative pathway of alcohol metabolism and is considered an intestinal stem cell signature gene. Although there is a slight difference between the basal expression level of *Aldh1a1* in *Cftr* $^{+/+}$ and *Cftr* $^{-/-}$ organoids, it was not significant at $p \leq 0.05$ (p=0.5258). The expression in response to treatment with LXR agonist GW3965 is drastically different (Figure 10).

Cftr $^{-/-}$ organoids respond to GW3965 by increasing the expression of *Aldh1a1*, however, this response is less than *Cftr*$^{+/+}$ organoids, but this difference is not significant at $p \leq 0.05$ ($p=0.4204$). The expression data of both *Scd1* and *Aldha1a1* show that the LXR agonist influences the stem cell compartment (organoids) and differential expression of *Cftr* has an effect either on the expression of these genes in response to treatment with GW3965 in organoids. Only one biological replicate was evaluated in this experiment. More replicates are needed to confirm or refute this result.

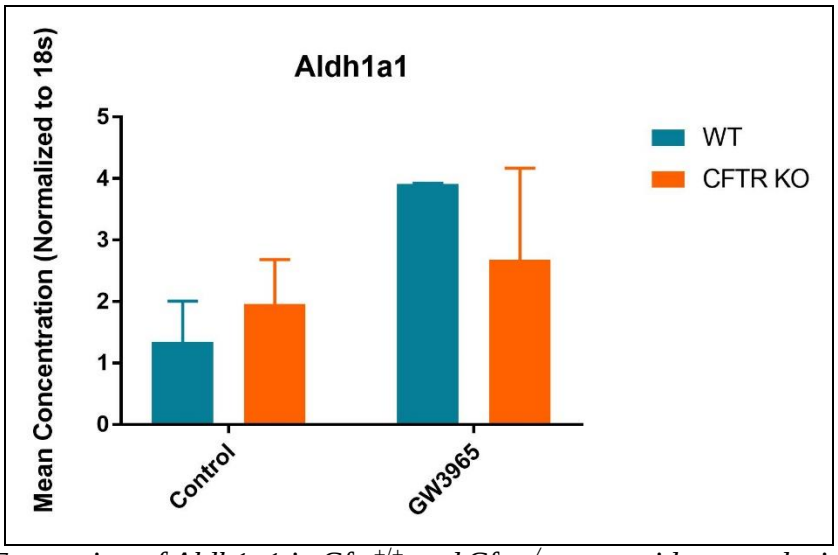

Figure 10. *Expression of Aldh1a1 in* Cftr$^{+/+}$ *and* Cftr $^{-/-}$ *organoids treated with GW3965.* The basal level of *Aldh1a1* expression is slightly increased in *Cftr* $^{-/-}$ organoids compared to *Cftr* $^{+/+}$ organoids. The expression of *Aldh1a1* in response to LXR/RXR pathway agonist GW3965 is stronger in *Cftr*$^{+/+}$ organoids than *Cftr* $^{-/-}$ organoids. The standard error for technical replicates is shown by the error bars.

We also analyzed expression of claudin 4 (*Cldn4*), an integral membrane protein that is a component of tight junction strands (Figure 11). As expected, *Cldn4* expression did not change due to treatment with LXR agonist GW3965, as it is not a target gene of the LXR/RXR pathway. Interestingly, the basal expression level of *Cldn4* is higher in *Cftr* $^{-/-}$ organoids, but this difference is not significant at $p \leq 0.05$ ($p=0.7172$).

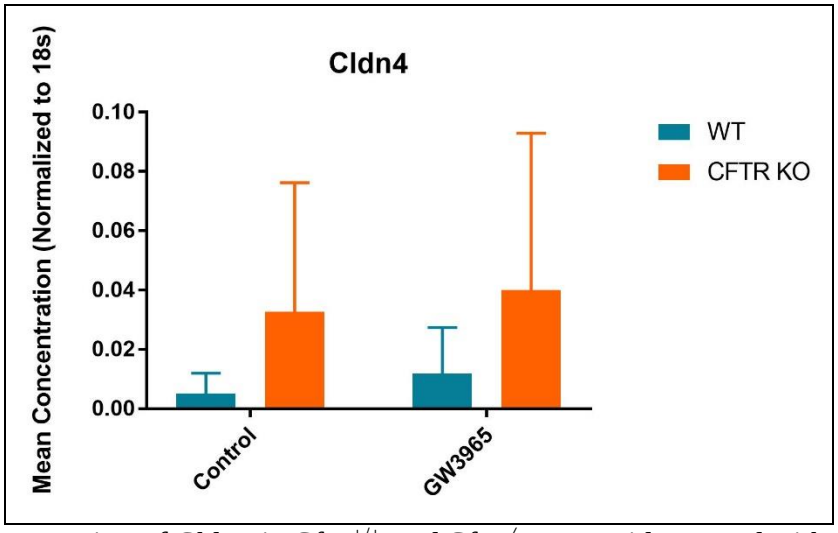

Figure 11. *Expression of Cldn4 in* Cftr $^{+/+}$ *and* Cftr $^{-/-}$ *organoids treated with GW3965.* The basal level of *Cldn4* expression is higher in *Cftr* $^{-/-}$ organoids compared to *Cftr* $^{+/+}$ organoids. The expression of *Cldn4* in response to LXR/RXR pathway agonist GW3965 does not change in *Cftr* $^{+/+}$ organoids and *Cftr* $^{-/-}$ organoids. The standard error for technical replicates is shown by the error bars.

To confirm the differences in basal expression levels of *Scd1* and *Aldh1a1*, we analyzed expression of these genes in *Cftr* $^{+/+}$ and *Cftr* $^{-/-}$ organoids derived from three distinct and separate pairs of littermate mice (Figure 12). Similar to the expression levels of the previous analysis, *Scd1* was expressed at a higher level in *Cftr* $^{+/+}$ organoids compared to *Cftr* $^{-/-}$ organoids, but this difference was not significant at $p \leq 0.05$ ($p=0.4577$, Figure 12a). *Aldh1a1* was expressed at a higher level in *Cftr* $^{-/-}$ organoids compared to *Cftr* $^{+/+}$ organoids, but again, this difference was not significant at $p \leq 0.05$ ($p=0.4478$, Figure 12b), which is consistent with the previous basal level expression data. This experiment was performed using only one biological replicate. More replicates must be obtained and evaluated to confirm or refute these results.

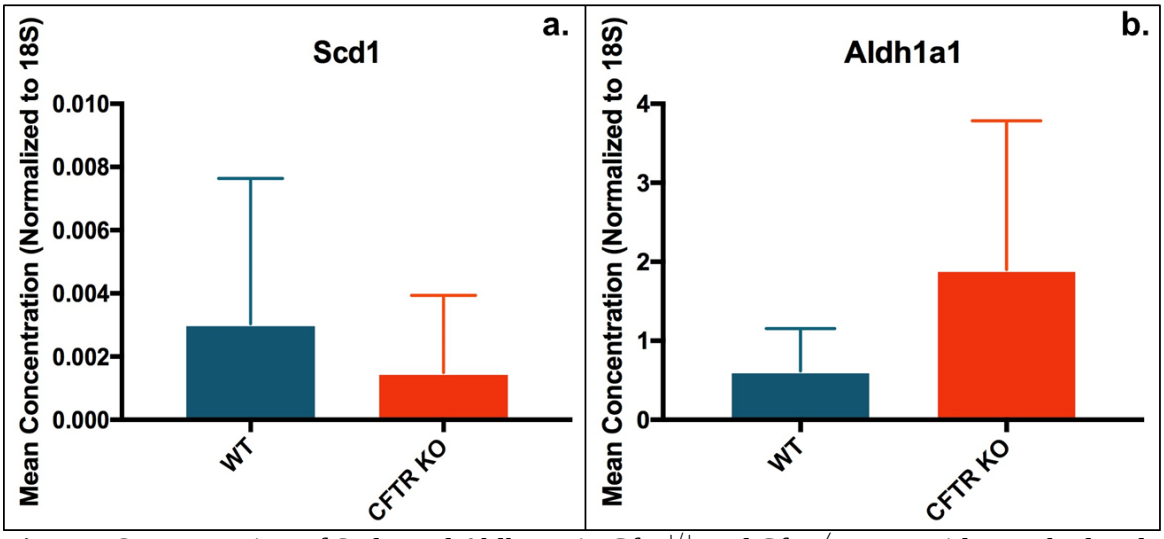

Figure 12. *Expression of Scd1 and Aldh1a1 in* Cftr $^{+/+}$ *and* Cftr $^{-/-}$ *organoids*. **a.** The level of *Scd1* expression is increased in *Cftr* $^{+/+}$ organoids compared to *Cftr* $^{-/-}$ organoids. **b.** The expression level of *Aldh1a1* is increased in *Cftr* $^{-/-}$ organoids compared to *Cftr* $^{+/+}$ organoids.

Discussion

The purpose of this thesis was to determine the role of *KCNQ1* and *CFTR* as colorectal cancer tumor suppressors by their regulation of the intestinal stem cell compartment. It was our goal to characterize the tumor suppressive mechanisms of these genes and their effect on the stem cell compartment by analyzing phenotypic differences and gene expression changes of organoids. Organoids are cultures of isolated intestinal stem cells that recapitulate the self-renewal and differentiation capacity of the tissue they are derived from. Thus, organoids provide a better physiological *in vitro* model than traditional monolayer culture techniques (Sato *et al.*, 2011). Our data support our hypothesis that loss of *KCNQ1* or *CFTR* influences changes to the intestinal stem cell compartment. Although our data does not provide a comprehensive mechanism by which

KCNQ1 or *CFTR* acts as a colorectal cancer tumor suppressor, the data does provide insight to possible biological pathways that may be involved.

Kcnq1 is expressed at the base of the colonic crypt

Our working model is that *Kcnq1* is a tumor suppressor by its effect on the regulation of the stem cell compartment. We analyzed the expression and localization of *Kcnq1* in the colonic tissue of mice by immunohistochemical analysis. *Kcnq1* is expressed at the base of the colonic crypt (Figure 1), with its expression diffusing until it is absent near the crypt-villus junction. The localization and expression of *Kcnq1* supports our hypothesis because it confirms that *Kcnq1* is expressed where the stem cells reside. There are an estimated four to six stem cells per crypt that express the intestinal stem cell marker *Lgr5* (Barker *et al.*, 2007). These stem cells are located immediately above Paneth cells in the small intestine, which are also located at the crypt base (Barker *et al.*, 2007). Because we confirmed that *Kcnq1* is expressed at the base of the crypt, where the stem cells reside, it is possible that *Kcnq1* exerts its tumor suppressive mechanism by influencing the stem cell compartment of the intestinal tissue, because it is spatially expressed in proximity to the stem cells. Our immunohistochemical analysis agrees with other previously published data by Preston *et al.*, who also showed that *Kcnq1* is expressed in the basolateral membrane of colonic crypt cells, and is not expressed near the top of the crypt (2011).

Organoids deficient in Kcnq1 or Cftr have increased cell viability

Previous data from our lab and collaborators defines *KCNQ1* and *CFTR* as human colorectal cancer tumor suppressor genes. We hypothesized that loss of either *Kcnq1* or *Cftr* in mice would affect the stem cell compartment of the intestinal tissue, and thus cause oncogenic phenotypes. To evaluate this, we harvested intestinal organoids from either *Kcnq1* $^{+/+}$ and *Kcnq1* $^{-/-}$ or *Cftr* $^{+/+}$ and *Cftr* $^{-/-}$ littermate paired mice. Organoids were used in this assay and throughout this thesis work to evaluate the effects loss of *Kcnq1* and *Cftr* had on the stem cell compartment specifically, since this is where colorectal cancer originates from. We analyzed the cell viability of these organoids using MTT, a colorimetric assay that measures the activity of cellular enzymes that convert the MTT dye to an insoluble blue form. Thus, the measured absorbency is representative of the number of viable cells in culture.

Kcnq1 $^{+/+}$ and *Kcnq1* $^{-/-}$ organoids were plated at four relative dilutions for the MTT assay (100, 75, 50, and 25). To analyze the absorbency data, the percent MTT signal was calculated by considering the WT "100" dilution as a value of one, and comparing the other values to this. In all four dilutions of organoids, the *Kcnq1* $^{-/-}$ organoids had a slightly higher percent MTT signal compared to the four respective dilutions of the *Kcnq1* $^{+/+}$ organoids (Figure 2a). This difference in MTT signal was less than 1.5-fold and was not statistically significant.

Cftr $^{+/+}$ and *Cftr* $^{-/-}$ organoids were also analyzed by MTT assay. These results are like that of *Kcnq1* organoids, in that the percent MTT signal is slightly higher (less than 1.5-fold difference) in all four dilutions of *Cftr* $^{-/-}$ organoids when compared to *Cftr* $^{+/+}$

organoids (Figure 2b). Although this difference is not statistically significant, it is a more pronounced difference than what was shown in comparable *Kcnq1* MTT data.

The results of this MTT analysis were not expected. We hypothesized that loss of *Kcnq1* or *Cftr* would cause oncogenic changes to the stem cell compartment, such as an increase in cell viability. Similar studies by a previous member of our lab, Dr. Bich Than, analyzed development of colonic organoids derived from *Kcnq1* $^{+/+}$ and *Kcnq1* $^{-/-}$ or *Cftr* $^{+/+}$ and *Cftr* $^{-/-}$ littermate paired mice (2014 and 2016, respectively). Colon organoids were harvested from a group of *Kcnq1* $^{+/+}$ and *Kcnq1* $^{-/-}$ age and gender matched mice and grown for five days, and organoid growth was monitored on days two through five. Than *et al.* found that loss of *Kcnq1* increased the number of colon organoids by more than three-fold, a statistically significant difference (2014). Than *et al.* performed a similar analysis in 2016 with *Cftr* $^{+/+}$ and *Cftr* $^{-/-}$ mice, and measured a 2.3-fold growth difference in organoids derived from *Cftr* $^{-/-}$ mice, a statistically significant result (2016). Considering this data, it was surprising that the MTT cell viability assay did not show greater differences between organoids derived from from *Kcnq1* $^{+/+}$ and *Kcnq1* $^{-/-}$ or *Cftr* $^{+/+}$ and *Cftr* $^{-/-}$ littermate paired mice. There are a few fundamental differences in the assays that may account for this discrepancy. While the studies by Than *et al.* showed a statistically significant increase in development of organoids due to loss of *Kcnq1* or *Cftr*, both analyses noted there were no obvious morphological differences between the KO and WT organoids. It is possible that the MTT assay is not sensitive enough to determine small differences in cell viability, and this may be reflected in our data. Another difference that may account for the discrepancy between the data is the organoids used in

Than *et al.*'s studies were derived from colonic tissue, while our organoids were derived from small intestinal tissue. Colorectal cancer arises from the colon, and while the small intestinal tissue physiology is comparable to the large intestine (colon), it is not the same. The difference in cell viability detected by MTT may more accurately reflect the differences in organoid development seen by Than *et al.* if the organoids used for the MTT assay were instead derived from colonic tissue. As these experiments were underway, we were also working to develop a protocol for the isolation and culturing of colonic organoids. This protocol is now established, and these experiments may be repeated in the future using colonic organoids.

Kcnq1 $^{-/-}$ *organoids exhibited a decreased unfolded protein response*

Loss of *Kcnq1* causes decreased activation of the unfolded protein response in intestinal organoids. Our initial analysis of organoid mRNA expression data obtained by Illumina Next-Generation RNA Sequencing utilized GSEA by the Broad Institute. GSEA allows the investigator to define biological or genetic phenotypes in a large expression dataset and compare the expression of predetermined gene sets to determine if a phenotype is enriched or depleted for those genes. We isolated mRNA from organoids derived from pairs of *Kcnq1* $^{+/+}$ and *Kcnq1* $^{-/-}$ age and gender matched mouse small intestine. This mRNA expression data was analyzed by GSEA, with the two phenotypes defined as *Kcnq1* $^{+/+}$ and *Kcnq1* $^{-/-}$. From this analysis it was determined that the unfolded protein response gene set is enriched in *Kcnq1* $^{+/+}$ organoids, and thus depleted in *Kcnq1* $^{-/-}$ organoids (Figure 4). This data suggests loss of *Kcnq1* expression affects either the

activation of the unfolded protein response in intestinal stem cell culture, or the response of the intestinal stem cells to activation of the UPR.

Although GSEA is informative, the conclusions that we draw from these analyses are limited. To further investigate the depleted expression of UPR genes in *Kcnq1* $^{-/-}$ organoids, we proceeded with functional assays. Organoids derived from pairs of *Kcnq1* $^{+/+}$ and *Kcnq1* $^{-/-}$ age and gender matched mice small intestine were treated with Thapsigargin, an inducer of the unfolded protein response. After treatment, RNA was isolated from treated and control organoids and analyzed by RT-qPCR. To determine if the unfolded protein response was activated in the stem cell compartment by Thapsigargin, we analyzed expression of UPR target genes *Atf4* and *Hspa5*. The increase in expression of these target genes upon treatment with Thapsigargin in both the WT and KO organoids (greater than 1.5-fold difference) indicated the treatment was inducing the UPR in organoids, as expected. *Atf4* is an activating regulatory element that is part of the unfolded protein response. *Atf4* causes transcriptional changes resulting in increases in protein folding, transport, and ER-associated protein degradation, while attenuating protein synthesis (Wang and Kaufman, 2014). There is no notable difference between the basal expression levels of *Atf4* in *Kcnq1* $^{+/+}$ and *Kcnq1* $^{-/-}$ organoids (Figure 5). However, after treatment with Thapsigargin and induction of the unfolded protein response, the expression of *Atf4* increases (more than 1.5-fold) in both *Kcnq1* $^{+/+}$ and *Kcnq1* $^{-/-}$ organoids. Comparison of the response of *Kcnq1* $^{+/+}$ and *Kcnq1* $^{-/-}$ organoids to induction of the UPR reveals that *Kcnq1* $^{-/-}$ organoids illicit a weaker response than *Kcnq1* $^{+/+}$

organoids, as the expression level of *Atf4* in Thapsigargin treated *Kcnq1* $^{-/-}$ organoids is less than that of *Kcnq1* $^{+/+}$ organoids.

Expression of *Hspa5* in *Kcnq1* $^{+/+}$ and *Kcnq1* $^{-/-}$ organoids showed a similar trend. *Hspa5* encodes the endoplasmic reticulum luminal glucose-regulated protein 78 (Grp78), which is an integral component of the unfolded protein response. Grp78 is a signaling regulator that binds to and maintains ER stress sensors PERK, ATF6, and IRE1. Upon ER stress, Grp78 is titrated away through binding to misfolded proteins, with allows the dimerization of PERK and IRE1 and triggers activation of their downstream signaling pathways (Lee, 2014). The basal expression levels of *Hspa5* is similarly low in both *Kcnq1* $^{+/+}$ and *Kcnq1* $^{-/-}$ organoids (Figure 6). After treatment with Thapsigargin and induction of the unfolded protein response, the expression of *Hspa5* increases (more than 1.5-fold) in both *Kcnq1* $^{+/+}$ and *Kcnq1* $^{-/-}$ organoids. Comparison of the response of *Kcnq1* $^{+/+}$ and *Kcnq1* $^{-/-}$ organoids to induction of the UPR reveals that *Kcnq1* $^{-/-}$ organoids illicit a weaker response than *Kcnq1* $^{+/+}$ organoids, as the expression level of *Hspa5* in Thapsigargin treated *Kcnq1* $^{-/-}$ organoids is less than that of *Kcnq1* $^{+/+}$ organoids. The difference between these two responses is less than 1.5-fold. It should be noted that the expression signal is very low. This may be due to the UPR being mostly restricted to the stem cell compartment, which represents only a fraction of the cells in an organoid.

These data suggest loss of *Kcnq1* influences the unfolded protein response in the intestinal stem cell compartment. The expression of UPR target genes *Atf4* and *Hspa5* in response to induction of the UPR by Thapsigargin was lower in *Kcnq1* $^{-/-}$ organoids compared to *Kcnq1* $^{+/+}$ organoids. Thus, loss of *Kcnq1* has an effect either on the

expression of these target genes in response to induction of the UPR, or on the response of organoids to the treatment with Thapsigargin.

Contrary to our data, previously established models of endoplasmic reticulum stress responses in cancer assert that many types of cancer cells increase expression of ER stress-related genes and proteins (Moenner *et al.*, 2007). The theory states that pathologic states (such as cancer) involve deregulation of ER homeostasis, and thus the ability of cells to handle these stresses conditions their intrinsic capacity to adapt for cell survival or enter apoptosis or senescence through ER-associated pathways (Xu *et al.*, 2005). Recent studies have demonstrated roles for UPR signaling in tumor growth and chemoresistance and that *in vivo* UPR activation is a crucial step during oncogenic transformation and cancer development (Wang and Kaufman, 2014). Interestingly, previous studies show Grp78 expression is increased in colon cancers (Moenner *et al.*,2007) and activation of BIP is correlated with high cell malignancy (Wang and Kaufman, 2014). Studies by Wang *et al.* (2012) and Madhevan *et al.* (2011) showed that during malignant progression, cancer cells activate pathways, such as the immune response, that may require UPR signaling to meet cellular needs by increasing folding and secretion of cytokines, angiogenesis factors, and extracellular matrix components. In addition to these intrinsic factors, rapidly dividing cancer cells are frequently required to thrive in hostile environments, which could also cause activation of the UPR by disruption of ER protein folding (Wang and Kaufman, 2014). Collectively, these data suggest a role, and possibly a requirement, of UPR activation in cancer cells.

Although the established model is that cancer cells exhibit increased UPR activation due to intrinsic and extrinsic stressors, our data show that loss of the tumor suppressor gene *Kcnq1* in intestinal organoids causes decreased expression of UPR target genes compared to wildtype organoids. The difference in these results could be due to general considerations that must be noted when studying the UPR in cancer. For example, the deletion of a gene may be activating in terms of the UPR for the first 24 hours, but detrimental for survival of the cell long-term. Thus, detailed kinetic studies analyzing multiple time points after gene knockdown are necessary to determine the full effect of loss of expression of a gene on the UPR. Another consideration to note is the induction of the UPR via pharmacological agents, such as Thapsigargin. This agent may have multiple effects on the cell, and thus physiologic challenges (such as hypoxia, nutrient deprivation, and reactive oxygen species) better model the environment of the cancer cell and can lead to different effects on the UPR.

Previous studies have demonstrated that UPR activation enhances the protein folding capacity of cancer cells to meet the demand for cell survival and protects cancer cells from stress-induced cell death (Wang and Kaufman, 2014). However, recent data have challenged this model, and may provide a better comparison for our own studies. Heijmans *et al.* found that UPR activation is involved in cell fate decisions and demonstrated that ER stress and UPR activation is low in intestinal stem cells (2013). This study also showed that activation of Perk-elF2α signaling alone is capable of inducing intestinal epithelial stem cell differentiation. These data suggest that the UPR may regulate intestinal epithelial stem cell differentiation. To further investigate how the

UPR regulates intestinal epithelial cell differentiation in a model that more closely resembles cancer, van Lidth de Jeude *et al.* analyzed cells that had acquired oncogenic mutations. van Lidth de Jeude found that loss of *Apc* alone, a common mutation in CRC, resulted in crypt elongation, activation of the Wnt signature, and accumulation of intestinal stem cells. This oncogenic phenotype was completely rescued upon activation of ER stress by additional deletion of *Grp78* (2016). In *Grp78 Apc* double knockout mice, stem cells were lost and repopulation of the stem cell population occurred by non-mutant cells only, which implies these double-knockout mice had lost the capacity to self-regenerate (2016). These data suggest a role for UPR activation in inducing stem cells to differentiate. Along this line, a decreased response to UPR activation could lead to maintenance of the stem cell phenotype in CRC. Heijmans *et al.* data supports this. They found that Thapsigargin-induced UPR activation caused repression of intestinal stem cell markers *Lgr5* and *Ascl2*.

To investigate this further, we analyzed the expression of *Lgr5* and *Ascl2* in organoids derived from one pair of *Kcnq1* $^{+/+}$ and *Kcnq1* $^{-/-}$ age and gender matched mice treated with Thapsigargin, and inducer of the unfolded protein response. Although the basal level of both of these stem cell markers was higher in *Kcnq1* $^{-/-}$ organoids, upon treatment with Thapsigargin, the expression of these markers drastically decreased (more than 1.5-fold) and in the *Kcnq1* $^{-/-}$ organoids, the expression of *Ascl2* and *Lgr5* was lower. This result suggests that upon ER stress, loss of *Kcnq1* has some effect on the stem cell compartment's differentiation and loss of stem-cell markers.

Our previous data show *Kncq1* is a tumor suppressor gene in CRC, and biological pathway analysis by gene expression data revealed loss of *Kcnq1* may be involved in the unfolded protein response. The experiments in this thesis confirm that loss of *Kcnq1* causes a decreased activation of the UPR upon induction of ER stress in the intestinal stem cell compartment. While these UPR experiments provide interesting data, it must be further explored and better understood. The UPR is an attractive target for drug discovery because of its inducible nature and demonstrated plasticity. However, it is apparent that loss of individual genes has unique effects on the UPR, and thus it is difficult to characterize how an entire tissue or organ will respond to UPR activation or suppression. It is also crucial to fully characterize the influence of the UPR on cancer cells, and if this influence is different at different stages of cancer development and progression. The exploratory work in this thesis provides a framework by which future studies can be focused on.

Cftr $^{-/-}$ organoids exhibited decreased LXR/RXR pathway activation

Loss of *Cftr* expression causes decreased activation of the LXR/RXR pathway in intestinal organoids. Previous work from our lab analyzed *Cftr* normal and deficient colon, small intestine, and tumors to determine what biological pathways were affected by loss of *Cftr* (Than *et al.*, 2016). IPA revealed *Cftr*-deficient normal and tumor tissue had a decreased activation of the LXR/RXR pathway. To further investigate the depleted activation of the LXR/RXR UPR pathway due to loss of *Cftr*, we proceeded with functional assays. Organoids derived from one pair of *Cftr* $^{+/+}$ and *Cftr* $^{-/-}$ age and gender matched mouse small intestine were treated with GW3965, an activator of the LXR/RXR

pathway. After treatment, RNA was isolated from treated and control organoids and analyzed by RT-qPCR. To determine if the LXR/RXR pathway was activated in the stem cell compartment by GW3965, we analyzed expression of LXR target genes *Scd1* and *Aldh1a1*. The increase in expression of these target genes upon treatment with GW3965 in both the WT and KO organoids (greater than 1.5-fold difference) indicated the treatment was activating the LXR/RXR pathway in organoids, as expected. We then proceeded to analyze target gene expression levels. *Scd1* encodes an enzyme that produces monounsaturated fatty acids, which are an important molecule for a multitude of biological processes. Its relation to cholesterol biosynthesis processes makes it a target of the LXR/RXR pathway. The basal expression level of *Scd1* was low and unchanged due to loss of *Cftr* in organoids (Figure 9). After treatment with GW3965, the expression of *Scd1* increased (more than 1.5-fold) in both *Cftr* $^{+/+}$ and *Cftr* $^{-/-}$ organoids. The expression of *Scd1* in response to treatment with GW3965 is significantly lower in *Cftr* $^{-/-}$ organoids compared to *Cftr* $^{+/+}$ organoids (more than 1.5-fold). This confirms the results of the IPA analysis of *Cftr* deficient tissue, which showed that loss of *Cftr* caused decreased activation of the LXR/RXR pathway.

Another target gene of the LXR/RXR pathway is *Aldh1a1*, a major enzyme in the oxidative pathway of alcohol metabolism. The basal expression levels of *Aldh1a1* were relatively unchanged due to loss of *Cftr* in organoids (Figure 10). In response to treatment with GW3965, the expression of *Aldh1a1* is significantly lower in *Cftr* $^{-/-}$ organoids compared to *Cftr* $^{+/+}$ organoids (more than 1.5-fold). This agrees with the *Scd1* expression data as well as the previously published IPA analysis (Than *et al.*, 2016), which showed

that loss of *Cftr* affects the response of the intestinal stem cell compartment to activation of the LXR/RXR pathway.

The LXR/RXR pathway was of initial interest to our lab as a potential biological pathway affected by the loss of *Cftr* not only because of its consistency as a finding in numerous expression analyses, but also because of its well-established involvement in cancer. Accelerated cholesterol and lipid metabolism are hallmarks of cancer, as proliferating cells increase cholesterol uptake due to the requirement for cholesterol in eukaryotic membranes (Gabitova *et al.*, 2014). Liver X receptors (LXR) are regulators of the cholesterol homeostasis network and coordinate growth with the availability of cholesterol (Gabitova *et al.*, 2014). Activation of the LXR/RXR pathway increases cholesterol efflux through ATP-binding cassette (ABC) class A transporters and thus decreases the amount of intracellular cholesterol (Gabitova *et al.*, 2014). Our data support a model whereby loss of the tumor suppressor gene *Cftr* in intestinal organoids causes decreased activation of the LXR/RXR pathway and leads to increased intracellular cholesterol. Increased cholesterol requirements is characteristic of rapidly proliferating and cancer cells.

The experiments in this thesis support the previously published IPA data that *Cftr*-deficient tissues exhibit inhibition of the LXR/RXR pathway. This conclusion may explain the functional mechanism of tumor suppression by *Cftr* in mouse intestinal stem cell compartments. Loss of *Cftr* expression either affects the activation of the LXR/RXR pathway in organoids or affects the response of the organoids to activation of the LXR/RXR pathway. It is important to understand if this inhibition causes increased

intracellular cholesterol levels overall, or if the tumor suppressive mechanism is not directly related to cholesterol levels in the cell. This model is important to pursue and characterize because nuclear receptors, such as LXR, are an important class of drug targets as their ligands easily pass biological membranes due to their lipophilic nature. If loss of *Cftr* causes oncogenic changes to the stem cell compartment through increase of intracellular cholesterol levels, it may be a promising target for drug development.

GSEA of human tumors determined loss of KCNQ1 or CFTR is related to enrichment of inflammatory pathway genes

To better understand which biological pathways were affected by loss of *KCNQ1* and *CFTR* in human colorectal cancers, we used GSEA to analyze biological gene sets that were enriched or depleted in the *KCNQ1* or *CFTR* low phenotype. Three sets of human colorectal primary tumor mRNA expression data were sorted continuously, from *KCNQ1* or *CFTR* low to high expression. GSEA (Broad Institute) was run on these expression datasets using the GEO Molecular signatures gene set "hallmarks of cancer." The top four gene sets that were determined as enriched in the *KCNQ1* low phenotype in all three colorectal tumor mRNA expression datasets are shown in Table 1. The *KCNQ1* low tumor phenotype was enriched in the following gene sets; epithelial mesenchymal transition, inflammatory response, allograft rejection, and interferon gamma response. The top four gene sets that were determined as enriched in the *CFTR* low phenotype in all three colorectal tumor mRNA expression datasets are shown in Table 3. The *CFTR* low tumor phenotype was enriched in the following gene sets; epithelial mesenchymal

transition, inflammatory response, TNF signaling via NF-κB, and angiogenesis. These gene sets represent biologically relevant groups of genes that share involvement in a specific biological pathway. Thus, it can be inferred that these pathways are enriched in the *KCNQ1* or *CFTR* low phenotype.

A majority of the gene sets enriched in the *KCNQ1* and *CFTR* low phenotypes are involved in the inflammatory response. Inflammation has long since been established as a colorectal cancer phenotype, and many studies suggest inflammatory mechanisms play a causal role in cancer development and progression. A study by McMillan, Canna, and McArdle in 2003 examined the relationship of the systemic inflammatory response and disease-free survival of CRC patients. They studied a total of 174 patients considered to have undergone curative resection and measured inflammatory response in these patients by recording circulating concentrations of C-reactive protein (CRP), a protein made by the liver and released into the blood upon inflammation (McMillan *et al.*, 2003). The study found that the presence of a systemic inflammatory response predicts a poor outcome in colorectal cancer patients who have undergone potentially curative resection surgery (McMillan *et al.*, 2003). More recent and detailed molecular studies show that many inflammation-associated genes, such as cyclooxygenase-2, nitric oxide synthase-2, and the interferon-inducible gene 1-8U are elevated in colonic neoplasms (Itzkowitz and Yio, 2004). Multiple knockout studies show that when inflammatory genes are disrupted, mice develop oncogenic phenotypes. For example, transgenic mice with disruption of *IL-10* develop adenocarcinomas after three and six months in 25 and 60% of the mice, respectively (Shattuck-Brandt *et al.*, 2000). A leading theory of how inflammation plays

a causal role in CRC development and progression is that the oxidative stress caused by chronic inflammation contributes to neoplastic transformation and a cancer-prone phenotype (Hussain *et al.*, 2003). Despite much effort, the mechanism of how inflammation causes CRC is not fully understood. The finding that inflammatory gene sets are enriched in both *KCNQ1* and *CFTR* low expressing human CRC tumors is a potential insight into the mechanism of tumor suppression by these two genes.

Another gene set significantly enriched in both *KCNQ1* and *CFTR* low expressing human tumor phenotypes was the epithelial-mesenchymal transition, a biologic process that allows a polarized epithelial cell in contact with the basement membrane to undergo multiple changes that enable it to transition to a mesenchymal cell phenotype (Kalluri and Weinberg, 2009). This cellular process is yet another well-researched area in which data supports its involvement in cancer. Epithelial-mesenchymal transitions represent an important source of mesenchymal cells that participate in pathological processes, such as tumor invasiveness and metastasis (Kalluri and Weinberg, 2009). Mesenchymal cells exhibit increased production of extracellular matrix components, increased resistance to apoptosis, and enhanced migratory capacity and invasiveness (Kalluri and Weinberg, 2009). Studies of immortalized human mammary epithelial cells by Mani *et al.* in 2008 showed that the induction of the epithelial-mesenchymal transition not only resulted in the acquisition of mesenchymal traits, but also the expression of stem-cell markers as well as the increased ability to form mammospheres and tumors more efficiently (Cell, 2008). Although comparable work has not been extensively performed for intestinal tissue, the GSEA results that low expression of both *KCNQ1* and *CFTR* in human tumor

tissue is associated with increased gene expression of epithelial-mesenchymal transition genes provides a possible mechanism for tumor suppression by these genes, and should be further explored.

GSEA of Kcnq1 $^{-/-}$ Organoids Revealed Similar Enrichment as Human Colon Tumors

We used GSEA (Broad Institute) to analyze changes in gene expression related to biological pathways in *Kcnq1* $^{+/+}$ and *Kcnq1* $^{-/-}$ organoids. We were interested to compare the GSEA analysis for *Kcnq1* $^{-/-}$ organoids compared to the GSEA analysis of human tumor tissue with low expression of *KCNQ1*. The enriched gene sets and their statistical values are reported in Table 2. The epithelial-mesenchymal transition gene set was enriched in the *Kcnq1* $^{-/-}$ organoids, similar to the enrichment of this gene set in both the *KCNQ1* and *CFTR* low-expression human tumor phenotype. Another common pathway enriched in both the *Kcnq1* $^{-/-}$ organoids and the *KCNQ1* low-expression human tumor tissues is the inflammatory response. Although the IL-6 JAK-STAT3 signaling pathway was found to be enriched in *Kcnq1* $^{-/-}$ organoids but not in the human tissue analysis, this gene set is involved in inflammation, which is consistent with the other gene sets upregulated in the analysis of human tissues. These similarities are interesting because they provide a qualitative analysis of the similarity between the two models: organoids derived from mice and human colon tumor tissue samples. The commonalities in enriched gene sets determined by GSEA allows us to confirm that our biological pathways of interest are of relevance in human tissues as well.

The cholesterol homeostasis gene set was enriched in the *Kcnq1* $^{-/-}$ organoids we analyzed. This finding is consistent with the well-established oncogenic phenotype found

in many types of cancers, due to the increased demand for cholesterol in rapidly proliferative cells. A dysregulation of cholesterol homeostasis was also found in previously published IPA analysis of *CFTR*-deficient tissues (Than *et al.*, 2016). Because *KCNQ1* and *CFTR* have interrelated functions in the intestinal epithelium, it is interesting but not surprising that knockout of one of these genes has interrelated and similar effects as the other.

Conclusions and Future Directions

Our preliminary data support a role for *KCNQ1* and *CFTR* as colorectal cancer tumor suppressor genes. The experiments in this thesis support our hypothesis that loss of *KCNQ1* or *CFTR* is related to changes of the intestinal stem cell compartment phenotype, or of organoids. Specifically, our data show that loss of *CFTR* expression has an effect on the LXR/RXR pathway response in organoids, and that loss of *KCNQ1* expression has an effect on the unfolded protein response in organoids. GSEA of human CRC tumor mRNA expression data revealed that both loss of *KCNQ1* and *CFTR* expression in these tissues affects many pathways, including the immune response and epithelial-mesenchymal transition. These responses may be implicated in the tumor suppressive function of *KCNQ1* and *CFTR*.

Further work must be completed to characterize the functional mechanism of tumor suppression by *KCNQ1* and *CFTR*. Firstly, the expression of *Cftr* must be characterized in the mouse colon. It is known that the protein is expressed in the intestinal epithelium, but it has yet to be determined if the protein is expressed in the base of the crypt, where the stem cells reside. This expression data would confirm our working

model of tumor suppression by *Cftr*, that the protein exerts its tumor suppressive effects on the intestinal stem cell compartment.

The phenotypic differences between *Kcnq1* and *Cftr* wildtype and knockout organoids must be further characterized. Although the MTT assay detected small differences between cell viability of the organoids, observational data suggests there are physical differences in the integrity of the organoids. Numerous times during the harvesting and plating procedure of intestinal organoids, we noticed the organoids derived from knockout tissue were more fragile and easily disrupted. Often, organoids derived from knockout tissues did not grow well in culture after being disrupted during the harvesting process. These observations suggest some sort of cell adhesion or cell integrity difference between wildtype and knockout tissues. This phenotype would be important to characterize because it may play a role in the metastasis and progression of CRC. To analyze these differences, immunohistochemical analysis of proteins known to have functional roles in cell adhesion and movement would be informative. Functional assays that involved mechanical disturbance of organoids and then colony forming analysis would also be useful. In general, understanding and fully characterizing the phenotypic differences between organoids derived from wildtype and knockout tissue (*Kcnq1* and *Cftr*) is a crucial step to understanding the tumor suppressive mechanisms of these genes.

Organoids were used in this thesis because they provide a physiologically relevant *in vitro* model. However, we discovered that replicating experiments with organoids was difficult, because they are such a direct representation of the tissue they are derived from,

and naturally, tissue characteristics vary from animal to animal. These differences must be reconciled and standardized by making cell stock lines to make organoids a more useful experimental model. Considering this, more functional assays are needed to further characterize the responses of organoids to agonists of specific pathways we are interested in, for example, the LXR/RXR pathway and the unfolded protein response. In addition, it would be informative to investigate the response of organoids to activation of the other pathways found in our GSEA, such as inflammation. There are many interesting assays possible that involve the immune response, but what would be most informative at this point is to fully characterize the changes in the immune response of organoids that do not express *Kcnq1* or *Cftr*.

Our data support the role of *KCNQ1* and *CFTR* as tumor suppressors in human colorectal cancers. Understanding the mechanism of tumor suppression could help develop more effective therapy for CRC. Gaining knowledge about the mechanism will also help identify at-risk individuals, and identify which individuals require more aggressive treatment and disease surveillance.

References

1. Baker, S. J., Markowitz, S., Fearon, E. R., Willson, J. K. V., and Vogelstein, B. (1990). Suppression of human colorectal carcinoma cell growth by wild-type p53. Science, 249, 912.
2. Barker, N. *et al.* (2007). Identification of stem cells in small intestine and colon by marker gene *Lgr5*. Nature 449, 1003-1007.
3. Barker, N. *et al.* (2008). The intestinal stem cell. Genes Dev. 22, 1856-1864.
4. Blackiston, D.J. *et al.* (2009). Bioelectric controls of cell proliferation: Ion channels, membrane voltage, and the cell cycle. Cell Cycle 21, 3519-3528.
5. Bos, J.L. *et al.* (1987). Prevalence of *RAS* gene mutations in human colorectal cancers. Nature 327, 293-297.
6. Bovenga, F., Sabbà, C., and Moschetta, A. (2015). Uncoupling nuclear receptor LXR and cholesterol metabolism in cancer. Cell Metabolism 21, 517-526.
7. Cao, S. S., and Kaufman, R. J. (2012). Unfolded protein response. Current Biology 22, 622-626.
8. Casimiro, M. C., Knollmann, B. C., Ebert, S. N., Vary, J. C., Greene, A. E., Franz, M. R., and Pfeifer, K. (2001). Targeted disruption of the *Kcnq1* gene produces a mouse model of Jervell and Lange–Nielsen Syndrome. Proceedings of the National Academy of Sciences 98, 2526-2531.
9. Cho, K. R., and Vogelstein, B. (1992). Genetic alterations in the adenoma–carcinoma sequence. Cancer 70, 1727-1731.
10. Clevers, H. (2006). Wnt/β-catenin signaling in development and disease. Cell 127, 469-480.
11. Dedek K, and Waldegger S. (2001). Colocalization of KCNQ1/KCNE channel subunits in the mouse gastrointestinal tract. Eur. J. Physiol. 442, 896-902.
12. de Jeude, J.V.L., Meijer, B.J., Wielenga, M.C.B., Spaan, C.N., Baan, B., Rosekrans, S.L., and Paton, A.W. (2016). Induction of endoplasmic reticulum stress by deletion of Grp78 depletes Apc mutant intestinal epithelial stem cells. Oncogene 36, 3397-3405.
13. De Lisle, R. C., and Borowitz, D. (2013). The cystic fibrosis intestine. CSH Perspectives in Medicine 3, a009753.
14. Demolombe S, Franco D *et al.* (2001). Differential expression of KvLQT1 and its regulator IsK in mouse epithelia. Am J Physiol Cell Physiol. 280, 359-372.
15. den Uil, S. H., Coupé, V. M., Linnekamp, J. F., van den Broek, E., Goos, J. A., Delis-van Diemen, P. M., and Medema, J. P. (2016). Loss of KCNQ1 expression in stage II and stage III colon cancer is a strong prognostic factor for disease recurrence. British Journal of Cancer 115, 1565–1574.
16. Diener, M. Hug, F., Strabel, D. and Scharrer, E. Cyclic AMP-dependent regulation of K+ transport in the rat distal colon. British Journal of Pharmacology, 118, 1477-1487.
17. Farin, H. F., Jordens, I., Mosa, M. H., Basak, O., Korving, J., Tauriello, D. V., and Clevers, H. (2016). Visualization of a short-range Wnt gradient in the intestinal stem-cell niche. Nature 530, 340-343.

18. Fodde, R., Kuipers, J., Rosenberg, C., Smits, R., Kielman, M., Gaspar, C., and Clevers, H. (2001). Mutations in the APC tumour suppressor gene cause chromosomal instability. Nature Cell Biology 3, 433-438.
19. Gorin, A., Gabitova, L., and Astsaturov, I. (2012). Regulation of cholesterol biosynthesis and cancer signaling. Current Opinion in Pharmacology 12, 710-716.
20. Harding, H. P., Novoa, I., Zhang, Y., Zeng, H., Wek, R., Schapira, M., and Ron, D. (2000). Regulated translation initiation controls stress-induced gene expression in mammalian cells. Molecular Cell 6, 1099-1108.
21. Jameson, J., & Loscalzo, J. Harrison's Principles of Internal Medicine, 19e.
22. Han, D., Lerner, A. G., Walle, L. V., Upton, J. P., Xu, W., Hagen, A., and Papa, F. R. (2009). IRE1α kinase activation modes control alternate endoribonuclease outputs to determine divergent cell fates. Cell 138, 562-575.
23. Haze, K., Yoshida, H., Yanagi, H., Yura, T., and Mori, K. (1999). Mammalian transcription factor ATF6 is synthesized as a transmembrane protein and activated by proteolysis in response to endoplasmic reticulum stress. Molecular Biology of the Cell, 10, 3787-3799.
24. Hodges, C. A., Cotton, C. U., Palmert, M. R., and Drumm, M. L. (2008). Generation of a conditional null allele for Cftr in mice. Genetics 46, 546-552.
25. He, X.C. *et al.* (2004). BMP signaling inhibits intestinal stem cell self-renewal through suppression of Wnt–bold beta-catenin signaling. Nature Genetics 36, 1117-1121.
26. Hussain, S. P., Hofseth, L. J., and Harris, C. C. (2003). Radical causes of cancer. Nature Reviews Cancer, 3, 276-285.
27. Itzkowitz, S. H., and Yio, X. (2004). Inflammation and cancer IV. Colorectal cancer in inflammatory bowel disease: the role of inflammation. Am. J. of Phys. Gastrointestinal and Liver Phys. 287, 7-17.
28. Jespersen, T., Grunnet, M., and Olesen, S. P. (2005). The KCNQ1 potassium channel: from gene to physiological function. Physiology 20, 408-416.
29. Kalluri, R. and Weinberg, R. A. (2009). The basics of epithelial-mesenchymal transition. The Journal of Clinical Investigation 119, 1420.
30. Kaser, A., Flak, M. B., Tomczak, M. F., and Blumberg, R. S. (2011). The unfolded protein response and its role in intestinal homeostasis and inflammation. Experimental Cell Research 317, 2772-2779.
31. Kaser, A. and Blumberg, R. S. (2010). Endoplasmic reticulum stress and intestinal inflammation. Mucosal Immunology 3, 11-16.
32. Kasper, D.L. *et al.* (2012). Harrison's Principles of Internal Medicine (19e.). McGraw Hill.
33. Kinzler, K. W. and Vogelstein, B. (1996). Lessons from hereditary colorectal cancer. Cell 87, 159-170.
34. Kunzelmann, K. (2005). Ion channels and cancer. The Journal of Membrane Biology 205, 159.
35. Lee, A. S. (2014). Glucose-regulated proteins in cancer: molecular mechanisms and therapeutic potential. Nature Reviews Cancer 14, 263-276.

36. Lin, C. Y. and Gustafsson, J. Å. (2015). Targeting liver X receptors in cancer therapeutics. Nature Reviews Cancer 15, 216-224.
37. Mahadevan, N. R., Rodvold, J., Sepulveda, H., Rossi, S., Drew, A. F., and Zanetti, M. (2011). Transmission of endoplasmic reticulum stress and pro-inflammation from tumor cells to myeloid cells. Proceedings of the National Academy of Sciences 108, 6561-6566.
38. Maisonneuve, P., Marshall, B. C., Knapp, E. A., and Lowenfels, A. B. (2012). Cancer risk in cystic fibrosis: a 20-year nationwide study from the United States. Journal of the National Cancer Institute 105, 122-129.
39. Mani, S. A., Guo, W., Liao, M. J., Eaton, E. N., Ayyanan, A., Zhou, A. Y., ...and Campbell, L. L. (2008). The epithelial-mesenchymal transition generates cells with properties of stem cells. Cell 133, 704-715.
40. McMillan, D. C., Canna, K., and McArdle, C. S. (2003). Systemic inflammatory response predicts survival following curative resection of colorectal cancer. British Journal of Surgery 90, 215-219.
41. Moenner, M., Pluquet, O., Bouchecareilh, M., and Chevet, E. (2007). Integrated endoplasmic reticulum stress responses in cancer. Cancer Research 67, 10631-10634.
42. Morokuma, J., Blackiston, D., Adams, D. S., Seebohm, G., Trimmer, B., and Levin, M. (2008). Modulation of potassium channel function confers a hyperproliferative invasive phenotype on embryonic stem cells. Proceedings of the National Academy of Sciences 105, 16608-16613.
43. Ni, M., and Lee, A. S. (2007). ER chaperones in mammalian development and human diseases. FEBS letters 581, 3641-3651.
44. Preston, P., Wartosch, L., Günzel, D., Fromm, M., Kongsuphol, P., Ousingsawat, J., ... and Jentsch, T. J. (2010). Disruption of the K+ channel β-subunit KCNE3 reveals an important role in intestinal and tracheal Cl− transport. Journal of Biological Chemistry 285, 7165-7175.
45. Reya, T. and Clevers, H. (2005). Wnt signalling in stem cells and cancer. Nature 434, 843-850.
46. Riss, T. L., Moravec, R. A., Niles, A. L., Duellman, S., Benink, H. A., Worzella, T. J., and Minor, L. (2016). Cell viability assays.
47. Saif, M. W., and Chu, E. (2010). Biology of colorectal cancer. The Cancer Journal 16(3), 196-201.
48. Sansom, O. J., Reed, K. R., Hayes, A. J., Ireland, H., Brinkmann, H., Newton, I. P., ... and Clarke, A. R. (2004). Loss of Apc in vivo immediately perturbs Wnt signaling, differentiation, and migration. Genes & Development 18, 1385-1390.
49. Sasso, G. L., Bovenga, F., Murzilli, S., Salvatore, L., Di Tullio, G., Martelli, N., ... and Palasciano, G. (2013). Liver X receptors inhibit proliferation of human colorectal cancer cells and growth of intestinal tumors in mice. Gastroenterology, 144(7), 1497-1507.
50. Sato, T. and Clevers, H. (2013) Growing self-organizing mini guts from a single intestinal stem cell: mechanism and applications. Science 340, 1190-1194.

51. Sato, T. *et al.* (2009). Single Lgr5 stem cells build crypt-villus structures *in vitro* without a mesenchymal niche. Nature 459, 262-265.
52. Shattuck-Brandt, R. L., Varilek, G. W., Radhika, A., Yang, F., Washington, M. K., and DuBois, R. N. (2000). Cyclooxygenase 2 expression is increased in the stroma of colon carcinomas from IL–10−/− mice. Gastroenterology 118, 337-345.
53. Sikandar, S.S. *et al.* (2010). NOTCH Signaling Is Required for Formation and Self-Renewal of Tumor-Initiating Cells and for Repression of Secretory Cell Differentiation in Colon Cancer. Cancer Research 70, 1469-1478.
54. Starr, T.K. *et al.* (2009) A Transposon-based genetic screen in mice identifies genes altered in colorectal cancer. Science 323, 1747-1750.
55. Starr, T.K. *et al.* (2011) A *Sleeping Beauty* transposon-mediated screen identifies murine susceptibility genes for adenomatous polyposis coli (Apc)-dependent intestinal tumorigenesis. PNAS 108, 5765-5770.
56. Subramanian, A., Tamayo, P., Mootha, V. K., Mukherjee, S., Ebert, B. L., Gillette, M. A., ... and Mesirov, J. P. (2005). Gene set enrichment analysis: a knowledge-based approach for interpreting genome-wide expression profiles. Proceedings of the National Academy of Sciences, 102, 15545-15550.
57. Than, BLN *et al.* (2013). The role of KCNQ1 in mouse and human gastrointestinal cancers. Oncogene 33, 3861-3868.
58. Than, B. L. N., Linnekamp, J. F., Starr, T. K., Largaespada, D. A., Rod, A., Zhang, Y., ... and Niemczyk, A. (2016). *CFTR* is a tumor suppressor gene in murine and human intestinal cancer. Oncogene 35, 4179-4187.
59. Todd, D. J., Lee, A. H., and Glimcher, L. H. (2008). The endoplasmic reticulum stress response in immunity and autoimmunity. Nature Reviews Immunology 8, 663-674.
60. Uno, S., Endo, K., Jeong, Y., Kawana, K., Miyachi, H., Hashimoto, Y., and Makishima, M. (2009). Suppression of β-catenin signaling by liver X receptor ligands. Biochemical Pharmacology 77, 186-195.
61. Vallon, V., Grahammer, F., Volkl, H., Sandu, C. D., Richter, K., Rexhepaj, R., ... and Lang, F. (2005). KCNQ1-dependent transport in renal and gastrointestinal epithelia. Proceedings of the National Academy of Sciences of the United States of America 102, 17864-17869.
62. van der Flier, L.G. and Clevers, H. (2009) Stem cells, self-renewal, and differentiation in the intestinal epithelium. Annu. Rev. Physiol. 71, 241-260.
63. Vedin, L. L., Gustafsson, J. Å., and Steffensen, K. R. (2013). The oxysterol receptors LXRα and LXRβ suppress proliferation in the colon. Molecular Carcinogenesis 52, 835-844.
64. Wang, M. and Kaufman, R. J. (2016). Protein misfolding in the endoplasmic reticulum as a conduit to human disease. Nature 529, 326-335.
65. Wang, S. and Kaufman, R. J. (2012). The impact of the unfolded protein response on human disease. J Cell Biol. 197, 857-867.
66. Warth, R., Alzamora, M. G., Kim, J., Zdebik, A., Nitschke, R., Bleich, M., ... and Kim, S. (2002). The role of KCNQ1/KCNE1 K+ channels in intestine and

pancreas: lessons from the KCNE1 knockout mouse. Pflugers Archiv. European Journal of Physiology 443, 822-828.
67. Xu, C., Bailly-Maitre, B., and Reed, J. C. (2005). Endoplasmic reticulum stress: cell life and death decisions. Journal of Clinical Investigation 115, 2656.
68. Yasuda, K., Miyake, K., Horikawa, Y., Hara, K., Osawa, H., Furuta, H., ... and Yamagata, K. (2008). Variants in KCNQ1 are associated with susceptibility to type 2 diabetes mellitus. Nature Genetics 40, 1092-1097.